Spring 2019

Behavior of Geothermal Energy Piles Embedded in Rock

Ehab Sabi
Southern Methodist University, esabi@smu.edu

BEHAVIOR OF GEOTHERMAL ENERGY PILES
EMBEDDED IN ROCK

Approved by:

Dr. Usama El Shamy
Associate Professor

Dr. Khaled Abdelghany
Professor

Dr. Brett Story
Assistant Professor

BEHAVIOR OF GEOTHERMAL ENERGY PILES EMBEDDED IN ROCK

A Thesis Presented to the Graduate Faculty of the

Lyle School of Engineering

Southern Methodist University

in

Partial Fulfillment of the Requirements

for the degree of

Master of Science in Civil Engineering

with a

Major in Civil Engineering

by

Ehab Sabi

(B.E., Civil Engineering, Jazan University, KSA)

May 18, 2019

ACKNOWLEDGMENTS

This work could not have been accomplished without the help and constant support of my advisor, Prof.Usama El Shamy, who guided my efforts and provided me with a major source of knowledge and expertise in the field. Also, he helped me in choosing the right topic in research, which taught me about so many things which I am really thankful for.

Secondly, I would like to thank my wife, parents, and friends who helped me a lot in finalizing this research within the limited time frame.

Sabi, Ehab (B.E., Civil Engineering, Jazan University, KSA)

Behavior of Geothermal Energy Piles
Embedded in Rock

Advisor: Dr. Usama El Shamy
Master of Science in Civil Engineering degree conferred May 18, 2019
Thesis completed May 4, 2019

Geothermal energy piles are categorized as closed systems. Energy piles are a relatively new technology which couples the structural role of traditional pile foundations to that of heat exchangers to fulfill the required energy demand of buildings and infrastructures. These foundations are equipped with pipes embedded in the concrete forming the pile. While connected to a heat pump, the fluid circulating inside these pipes provides the exchange of heat with the ground for heating and cooling purposes. As the undisturbed temperature at the shallower depths of the ground stays comparatively constant the whole year, being warmer than the surrounding temperature in winter and cooler in summer, the capacities of ground thermal storage are beneficial for withstanding the process of cooling and heating. In this study, heat exchange between the pile foundations and rock is investigated. The behavior of such foundation as energy piles, which are governed by their response to thermo-mechanical loads, is presently not fully understood. The influence of different pipe configurations embedded in the pile is examined while the pile is embedded in two different rock types (limestone and sandstone). It has been observed that pipe configurations strongly affect the behavior of the energy piles. An increase in the axial distributions of vertical thermal stresses has been recorded when the pile equipped with double U-pipes is compared with that of the single U-pipe configuration. The maximum value of the axial distributions of the thermal vertical displacements was observed when the pile foundation equipped with double U-pipes was buried in the limestone.

TABLE OF CONTENTS

LIST OF FIGURES

LIST OF TABLES

Dedicated to my brother Osama Sabi [1989 2014]

Chapter 1

INTRODUCTION

1.1. Objectives and Motivation

The constant demand for clean energy to serve for sustainable development made geothermal energy the perfect source to be used for getting clean and renewable energy. However, Geothermal energy is environmentally friendly because extraction of its energy does not cause carbon dioxide which can pollute the environment in comparison to fossil fuel energy extractions in terms of processing and operations. Geothermal energy systems do not require transport or storage of polluting or hazardous substances. It does not contribute any issues on a human scale. Moreover, this energy can be available 24 hours a day and it does not depend on climatic conditions. Economically, geothermal energy is one of the most cost-effective forms of renewable energy. It contributes for achieving the Independence of energy for electric power production. Geothermal energy can help to ensure energy independence and eliminate the use of fossil fuels for electric power production which already happened in volcanic islands such as Dominica. Recently, the Caribbean islands are almost entirely dependent on fossil-based energy.

Nowadays, there are many purposes of using geothermal energy systems which are heating and cooling buildings and residential houses, air conditioning, electric generations, hot water production for bathing and kitchens, agricultural purposes, and industrial uses. There are a lot of benefits of using geothermal systems: i) covering electricity needs of the desired area, ii) reduce and stabilize the electricity cost, iii) in the long run, geothermal energy systems could help to avoid production of tons of CO_2 into the atmosphere annually, iv) it can help to generate additional revenue for the national budget in proportion to the amount of electricity exported to cities and villages, v) guarantee at least part of the economic development of

new cities, especially in the big cities which are created and designed be a tourist spots in the region. Geothermal energy projects will contribute to creating several hundred direct and indirect jobs during the construction phases and operation of the power stations, vi) reduce the cost of the kWh and significantly will limit the need to import hydrocarbons, vii) geothermal energy will help to provide local taxes for the national budget, ix) geothermal energy could keep individual houses and the local companies self- dependent on the air conditioning and electricity, x) it will carry a new dynamic to the local economy.

1.2. Geothermal Energy Systems

The global energy crisis leads to the need to use renewable energy, such as geothermal energy. Geothermal energy is a form of thermal energy which generated in the core of the earth about 600 km under the ground. Temperature hotter than the surface of the sun is constantly generated inside the earth because of radiogenic decay of naturally occurring isotopes and because of that it is a renewable energy. The temperature inside the earth which is at the core of the earth can reach up to 5000°C. However, it decreases gradually as moving from the core of the earth towered the surface to reach around 10°C. This gradient of temperature drives a continuous flux of thermal energy which is from the core of the earth to the surface, in the format of a wide range of energy sources. The source range for geothermal energy are from the shallow, intermediate, and deeper depths. The shallower depths start from the order of the ten's meters to the few hundred meters, and the intermediate depths start from the edge of shallower depths to the order of kilometers to the deeper depths with extremely high temperatures of molten rocks 2.1. Geothermal energy systems consist mainly of two types which are shallow geothermal energy and deep geothermal energy. This study will focus on shallow geothermal energy, and will be referred to herein as geothermal energy systems [3].

Nowadays, the crisis of fossil fuel made geothermal energy systems so important. There are a lot of advantages of using geothermal energy over conventional fossil fuel resources. Geothermal energy systems are suitable methods to reduce carbon dioxide emissions. It is a

renewable heat source and economic source. Basically, there are two limitations which are availability and cost. For example, deep geothermal energy required abundant geothermal resources; generally, areas with recent tectonic activity. There is a high risk of failure on establishing deep geothermal systems because the cost is quite high compared with shallow geothermal energy. For instance, a little difference in the temperature of the extracted water from the reservoir can cost a huge loss of investment. However, geothermal energy normally can be generated by drilling deep holes into the earth. There are two types of extractions which are open and closed systems [3]. The Schematic of the systems can be seen in Figure 1.1.

1.2.1. Open Systems

The terminology of open systems is that the energy is created by pumping the water through the reservoir, where it will be circulating through hot fractured rock. After that it will be collected on the other side in order to bring it back to the surface as shown in Figure 1.2. An open system mainly depends on ground water wells in order to extract or inject water to/from water bearing layers in the underground (aquifers). Technically, an open system requires two wells: one can be used to extract the water from underground and the other one to inject it to the same aquifer [3]. In fact, an open system provides a powerful heat source with low cost. In contrast, it requires maintenance and a suitable aquifer that satisfies the requirements listed below:

1. Adequate permeability is needed to allow production of the required amount of ground water with small drawdown.

2. The chemistry of groundwater should be good which contain low iron to avoid issues with corrosion, scaling, and clogging.

Open systems can be suitable to use for big installations. The most powerful ground source heat pump system is located in Louisville, Kentucky, USA which uses groundwater wells to supply ca. 10 MW of heat and cold to a hotel and offices [73].

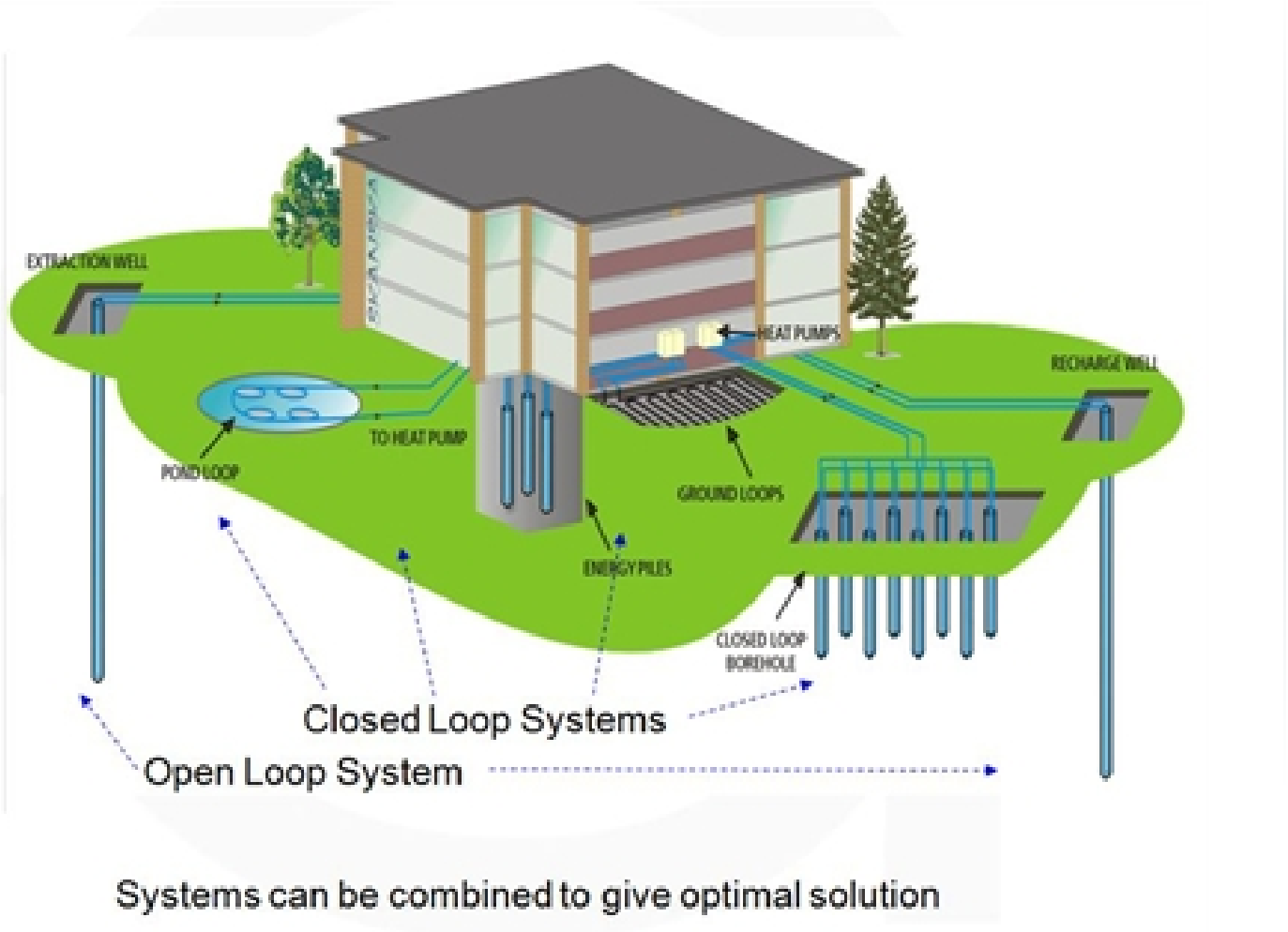

Figure 1.1. Schematic of Geothermal Energy Systems [9].

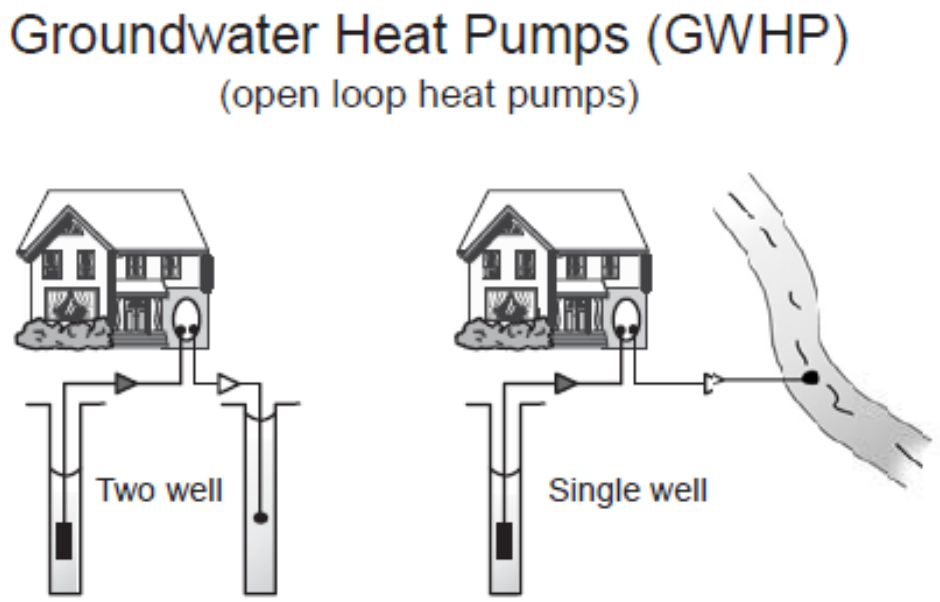

Figure 1.2. Schematic of an Open System [20].

1.2.2. Closed Systems

A closed system is about a single pipe where the water is bumped in one direction (Entrance path) and going to the other direction (exiting path) of the same pipe as shown in Figure 1.3. The implementation of closed systems can be done in many ways which are in horizontal and vertical directions see Figure 1.4, but it depends on several factors [3]. The most important factors are the geothermal energy sources and enough area to accommodate the system. The closed system can be divided into several types such as heat pips, direct evaporation bore-hole heat exchangers, bore-hole heat exchangers (BHEs), horizontal collectors, geothermal energy baskets, and thermal piles. Each type has its own configuration, the required space, and installed depths of these systems. The terminology of a closed system is a network of pipes, which are buried underground which function as heat exchangers. The popular materials are used for the pipes are mostly high-density polyethylene (HDPE), steel, and copper [20].

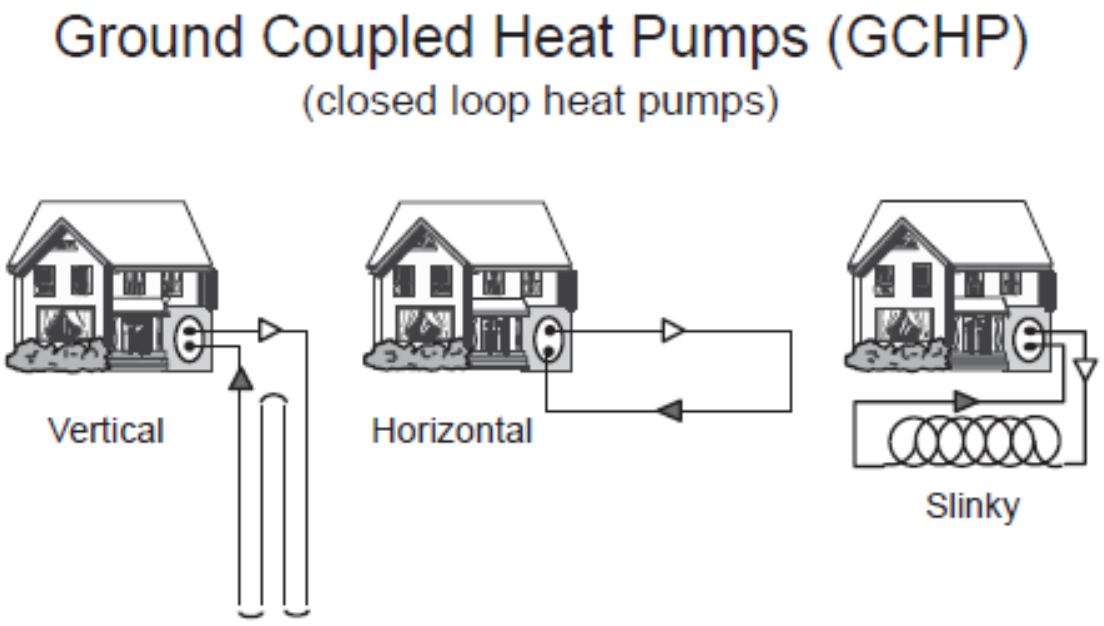

Figure 1.3. Schematic of a closed system [20].

1.3. Shallow Geothermal Energy

Shallow geothermal energy systems provide a great source of thermal energy that can be used for heating and cooling of buildings and companies because it is a renewable source of energy. Heat transfer due to temperature gradient between the bottom of the earth and the air is occur continuously. At approximately 10 m under the ground, the seasonal temperature variation is decreased to a constant temperature of around 12°C. Going from the surface of the earth towards the bottom of the earth, the temperature is known to increase with an average gradient of 3°C per 100 m depth. The first 100 m is suitable for storage and supply of thermal energy, even though there is a relative low temperature because the thermal interaction between the earth and the air. Two utilized energy systems are ground source heat pumps and underground thermal energy storage [58].

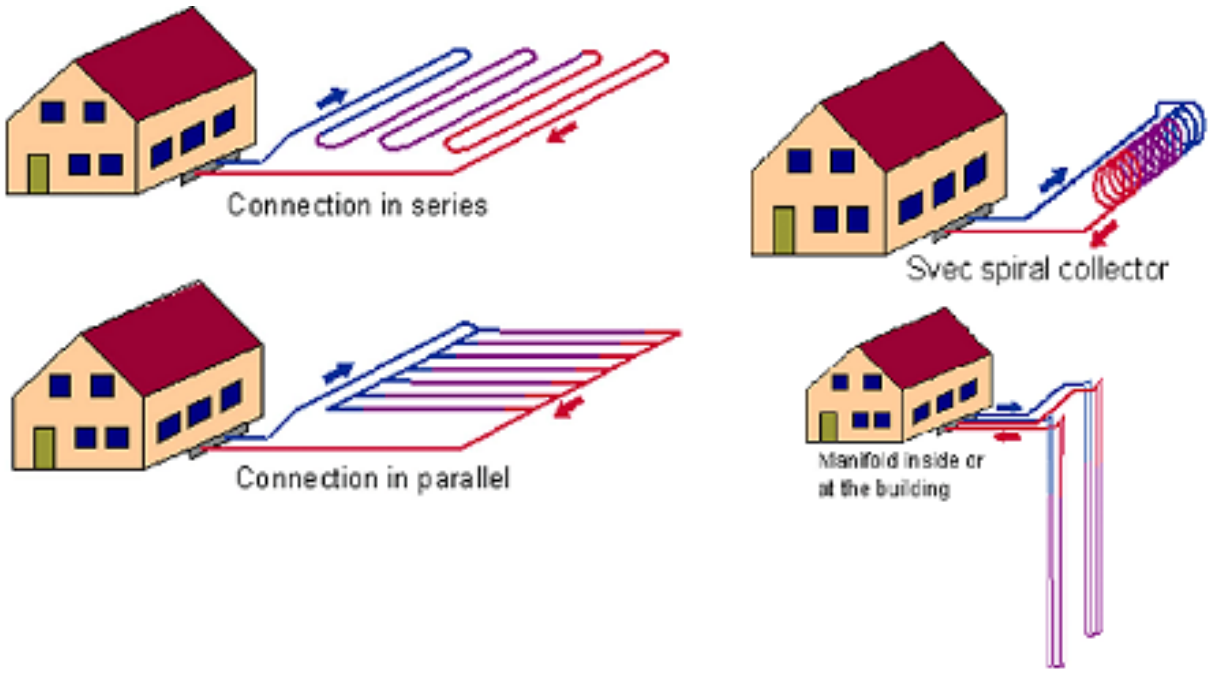

Figure 1.4. Schematic of Vertical and Horizontal Closed Systems [72].

1.3.1. Ground-Source Heat Pumps

Ground source heat pump (GSHP) is also known as a geothermal heat pump and down-hole heat exchanger (DHE). All are geothermal systems which are mentioned above as open and closed systems and can be seen in Sections 1.2.1 and 1.2.2, respectively. However, the open system is also known as a doublet which function to extract heat from groundwater and carry it to the surface of the earth by using at least two separate wells. Practically, one of the wells will be used for extracting the groundwater, and the second is for re-injecting the groundwater. This system is around eight times more efficient than closed systems.

The idea of a closed system is to extract the heat from the earth by installing pipes containing a fluid (which it can be water) embedded in the soil mass or rock. The fluid will be circulating inside the heat exchanger pipe until reaching a heat pump at the surface inside a proper place such as a building. The heat pump will collect and transport the heat from the fluid to the heating system. The great thing about the closed systems is that it does not

require an aquifer and one bore-hole is enough for the extraction of thermal energy. Closed system can be installed ether vertically or horizontally.

The vertical system is more popular than the horizontal systems and widely used especially in places where the area is limited. The system is known as bore-hole heat exchanger (BHE) or down-hole heat exchangers. However, the configuration of pipes varies which includes U pipe, UU pipes, or W pipe, and are fixed by several materials such as concrete, soil, rock, or grout. The material that is used for the pipes is mainly plastic, i.e. polyethylene or polypropylene.

As mentioned earlier the heat pump is located inside buildings. The function of the heat pump is to extract required amounts of heat from the fluid and pumps it back to the BHE. Sometime, the fluid used such as water is mixed with 20–25 % anti-freezing coolant such as Mono Ethylene Glycol to stop the fluid from freezing and sometimes it will get in contact with the surrounding materials (soil,rock) via the U-tube material and the grout. The grout is usually Bentonite-Cement mix.

Finally, the heat pump effectiveness can be described as a number called the coefficient of performance (COP) [74], which is the ratio of the heat transferred into the system to the work required to transfer that heat described as

$$COP = \frac{heat\ transferred}{work\ done\ by\ pump} = \frac{Q}{W} \tag{1.1}$$

For example, if the work needed to raise 1 kWh of heat is 0.25 kWh, the result of the coefficient of performance is 4, which means that the heat transferred to the building is four times greater than the work done by the motor of the heat pump. Moreover, the typical number of the coefficient of performance is usually ranging from 3.5 to 4, which is at the starting of the heating season, where the good values of the coefficient of performance are 5 or 6 for both heating or cooling systems [74]. The extraction can cause a drop in the ground temperature which will lead to a decrease in the coefficient of performance.

1.3.2. Underground Thermal Energy Storage

The shallower depth of the earth is suitable for storing energy, and getting more attention as colds and hot water stored in the ground can be used for cooling and heating of buildings the entire year. There are two systems as we mentioned in Sections 1.2.1 and 1.2.2; open which is known as aquifer thermal storage and closed, which is known as duct thermal storage or bore-hole storage [22].

1.3.2.1. Aquifer Thermal Energy Storage

Aquifer Thermal Energy Storage (ATES) is an open system which depends on the heat carried by the groundwater. The system is usually installed in porous aquifers with medium to high permeability and transmissivity. As mentioned in Section 1.2.1 the system requires a minimum of two wells, one for the warm water and the other for cold water. In summer, the cold water is used for cooling, and the resulting hot water is stored in the warm reservoir. In winter the process is flipped. The disadvantage of this system is that, it is good only in places with permeable aquifers. However, this system is environmentally safe. The used water cannot be contaminated because it does not mix with other fluids. Furthermore, the extracted water is the same as the re-injected water, which means that there is no loss of the groundwater [3].

1.3.2.2. Duct Thermal Energy Storage

Duct Thermal Energy Storage (DTES) is described as a closed system. This system can be implemented in varying configurations as mentioned in Section 1.2.2. Typically, bore-hole depths from 20-50 m are drilled where plastic pipes are installed as heat exchangers and carry the fluid. The thermal energy will be extracted from the fluid while circulating inside the pipes. The characterization of this system is that the pipe network and fittings are less exposed to scaling and clogging as compared to the ATES. However, the efficiency of this system depends on many factors such as geology, temperature gradient of the earth, groundwater conditions, and the thermal properties of the ground (soil, rock) [3].

1.4. Geothermal Energy Piles

The geothermal energy pile is a closed system configuration. Energy pile is a new technology which couples the structural role of traditional pile foundations to that of heat exchangers to fulfill the required energy of buildings and infrastructures. These foundations are equipped with pipes embedded in the concrete which are full of fluid circulating inside to exchange heat with the ground for heating and cooling purposes, especially when they are connected to heat pumps. In these studies, heat can be exchanged between the foundation and the rock, as the undisturbed temperature at the shallower depths of the ground stays comparatively constant the whole year. Being warmer than the surrounding temperature in the winter and cooler in the summer, in both media, the capacities of thermal storage are beneficial for enduring the process. The energy piles will be connected to the geothermal heat pump and can carry the stored heat and their energy input into buildings during the heating season and vice versa. During the cooling season, the heat can be extracted from the conditioned spaces and inject it (again, in addition to their energy input) to the rock. The using of energy pile foundations have been increasing world-wide because of the savings in the installation costs related to their hybrid character and to the drilling processes [19].

1.5. Thesis Outline

This work will investigate the geothermal energy pile, which involves a closed system buried in rock and soil materials. A literature review in Chapter 2 will present the history of the geothermal energy, shallow geothermal energy, and geothermal energy piles. The finite element modeling of the examined problem is first presented in Chapter 3 and their results will be outlined in Chapter 4. In Chapter 5, the thermo-mechanical behavior of the energy piles and the related energy and geotechnical performances are discussed with reference to the simulated design solutions.

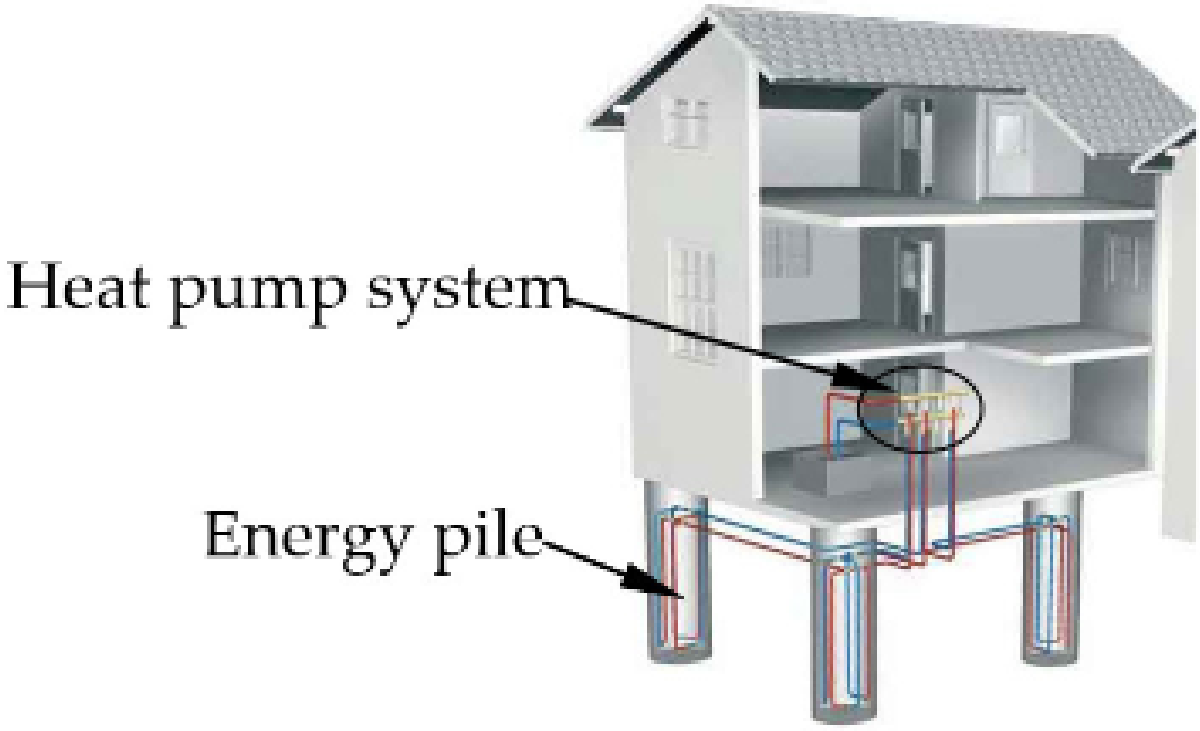

Figure 1.5. Schematic of Energy Piles in a Building [9].

Chapter 2

LITERATURE REVIEW

The geothermal energy techniques are mainly used to extract heat from the earth. It is known that heat is a form of energy [20]. Geothermal energy can be found from two different sources which are solar radiation and terrestrial heat flows [42]. The two sources can be exploited to various extents which depend on the geothermal installation depth. The surface of the earth and the atmosphere are heated by solar radiation. This energy will be transferred into the ground by the movement of the seepage water. The balance of the heat is essentially governed by a heat source known as solar energy zone.

2.1. Brief Description of Geothermal Energy

The existence of volcanoes, hot springs, and other thermal phenomena led people to think that the bottom of the earth is hot, but the first representation of a hot earth was not until a period between the sixteenth and seventeenth century, when people dug up few hundreds of meters underground for the first mines. The conclusion drawn from our ancestors is that the temperature of the earth increased with depth.

The thermometer was probably the first device for the measurements of heat in a mine near Belfort, France in 1740 [14]. Modern scientific technics and methods were being used for the thermal regime of the earth. However, those things did not start until the twentieth century which the role played by radiogenic heat had been discovered that led humankind better understanding such phenomena as heat balance and the Earth's thermal history. The heat continually generated by the decay of the long-lived radioactive isotopes of uranium (U^{238}, U^{235}), thorium (Th^{232}) and potassium (K^{40}), which are present in the Earth, must be taken into account in all modern thermal models of the Earth [15, 54].

The continental mainland has an average terrestrial heat flux of about 0.07 Wm^{-2} provided from the gravitational energy and radioactive deterioration together. The energy is transported from the crustal and sub-crustal regions to shallow depths which near the surface of the Earth. The main mechanisms behind this transfer of heat are conduction and convection [15]. The way geothermal energy installations work can be crucially affected by condition and convection. The effect of the energy transport controlled by phonon radiation at deep depths within the earth is negligible because at this depth transport becomes effective only at temperatures higher than about 700 °C.

As going from the surface toward the core of the earth, temperature increases with the depth. This rise is described by the geothermal gradient, which on average is about 2.5-3 °C per 100 m.

The equation below describes the relationship between temperature gradient θ (k . m^{-1}), the thermal conductivity λ (W . m^{-1} . k^{-1}) and the heat flux q_{sp} (W . m^{-2})

$$q_{sp} = -\lambda \cdot \left(\frac{\partial T}{\partial x} + \frac{\partial T}{\partial y} + \frac{\partial T}{\partial z} \right) \tag{2.1}$$

Where:

q_{sp} = specific heat flux (W . m^{-2}),

λ = thermal conductivity (W . m^{-1} . k^{-1}),

T = absolute temperature (K),

x, y, z = spatial coordinates (m)

The difference of the temperature magnitude is essentially important for the thermal conduction. The heat transfer path length is considered through the body of rock and the parameters of the rock. Thermal conduction can be classified as steady or unsteady. The steady case (conductive), where the thermal conductivity λ is the only critical rock parameter when quantifying the heat transfer. Fundamental here is Fourier's law, whose differential, general form for homogeneous solid bodies in its first derivative is as follows in Equation 2.1 [20].

The primordial energy of planetary accretion are the other potential sources of heat which could be added to the radiogenic heat. In those of modules, they were not realistic theories until 1980s. However, it was demonstrated that our planet is slowly cooling down, and that there was no equilibrium between the radiogenic heat generated in the Earth's interior and the heat dissipated into space from the Earth [20].

An example of this phenomena can be explained in the study of Stacey and Loper [75]. The total flow comes from the Earth is estimated to be 42×10^{12} W (conduction, convection and radiation) which 8×10^{12} W provided from the crust. It represents only 2% of the Earth total volume which it is rich in radioactive isotopes. However, the mantle represents 82% of the heat which is 32.3×10^{12} W and the heat that comes from the core is 1.7×10^{12} W, that represents only 16% of the total volume but it does not have radioactive isotopes. Figure 2.1 shows the schematic of the inner structure of the Earth [75]. According to Dickson [20], the rate of the cooling of the mantle the Earth is estimated to be 10.3×10^{12} W, since the radiogenic heat of it is estimated to be at 22×10^{12} W [51].

In the greater number of recent estimated data, the heat flow from the Earth is about 6% higher than the number that is used by Stacey and Loper (1988). However, the operation of cooling is still slow. The mantle temperature has reduced no more than 300 to 350 °C in 3 billion years, but still at its base is about 4000 °C. The total heat content of the Earth which is above a supposed average surface temperature of 15 °C seems to be of the order of 12.6×10^{24} MJ, and that of the crust is of the order of 5.4×10^{21} MJ [5].

Recently, the utilization of the geothermal energy is world widely imported and offer new perspectives in this sector. However, in the first of the nineteenth century, the energy content was already being exploited in geothermal fluids. In that period of time, a chemical industry was established in Italy in a place called Larderello to extract boric acid from the hot waters naturally or by drilled shallow bore-holes. Evaporating the hot fluids in iron boilers by using the wood as fuel was the way how to provide boric acid at that time. In 1827, the creator of that industry established an innovative system for using in the evaporation processes by using the heat of the boric fluids rather than burning wood from the forests. The utilization

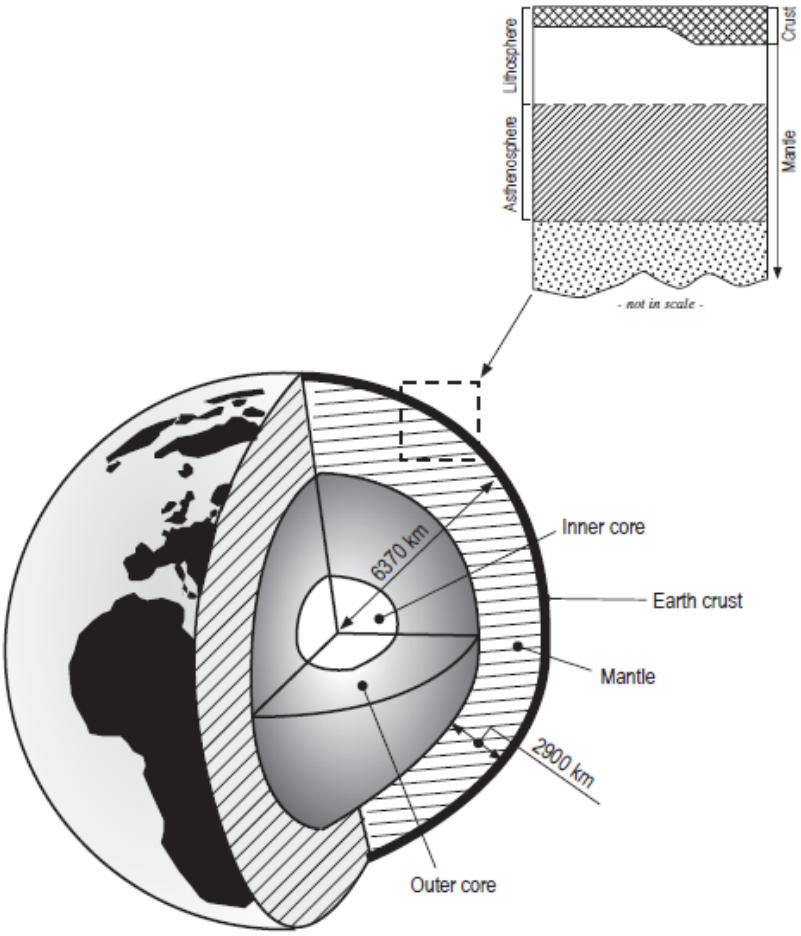

Figure 2.1. Schematic of the Earth's core, mantle and crust Source Source: Dickson and Fanelli *et. al* [20].

of natural steam to exploit its mechanical energy started during this time. Furthermore, in the period between 1850 and 1875 at Larderello, the factory held the monopoly for boric acid production in Europe. The low-pressure steam existed to be used to heat industrial and residential buildings and greenhouses in the Tuscany area between 1910 and 1940. Also, in 1928, Iceland (which is the pioneer in the exploitation of the geothermal energy) started utilizing its geothermal fluids specially hot waters for domestic heating [20]. The first use for the geothermal steam occurred in 1904 in Larderello, Italy to generate electricity. After by 1942, the capacity of the combined geothermo-electric energy had reached 127,650 kWe. Later many countries followed the example set by Italy. In 1919, the first geothermal wells in Japan were drilled at Beppu, and shortly after Geysers, California, US in 1921. A small geothermal power plant began its operations in New Zealand in 1958, and in 1959 in Mexico. Expansion of this type of energy source began in 1960 in the United States, and so many more countries in the years to follow [20].

After WWII, so many countries started importing geothermal energy systems which were considered to be economically competitive when comparing with other forms of energy such as fossil fuel. According to the Huttrer study that was conducted in 2001, geothermal electric capacity increased from 6,833 MWe in 1995 to 7,974 MWe in 2000 [39]. In addition, the same study showed reports on the overall installed capacity in 2004 (8,806.45 $M4We$). By considering the Huttrer study, the geothermal energy power installed in developing countries in 1995 (38%) and 2000 (47%) of the world total, see Table 2.1 which presents the countries that utilize geothermal energy to generate electricity. Another study was conducted by Dickson in 1988 showed that the utilization in some developing countries of geothermal energy have exhibited an interesting trend over the years. In the time between 1975 and 1979 the electric capacity of geothermal energy installed in those countries raised from 75 to 462 MWe; by the end of 1984, this result had accomplished 1495 MWe. However, the rate of increasing is available during these two periods which are 500% and 223%, respectively. It was a remarkable growth of almost 150% in the period from 1984 to 2000 [21].

In addition, in some areas, geothermal power plays an important role in the energy balance specially in the developing counties as can be seen in Table 2.1, which demonstrates the geothermal power percentage according to the total power of electricity that performed in some of these countries, relative to 1998.

Table 2.3 shows the installed energy and capacity used worldwide for the year 2000 which are 190,699 TJ/yr and 15,145 MWt, respectively. Table 2.3 reports the direct use of the fifty-eight countries compared to the twenty-eight in 1995 and the twenty-four in 1985. However, heat pumps are the most popular nonelectric used worldwide in term of the installed capacity which about 34.8%, followed by bathing 26.20%, space heating 21.62%, greenhouses 8.22%, aquaculture 3.93%, and industrial processes 3.13% [55].

2.2. Brief History about Energy Pile

The utilization of geothermal energy becomes worldwide popular. The energy performance of buildings highly encourages consolidation of applications of energy from renewable sources which recently was adopted European Parliament (2010/31/EU) [66]. The growth of the renewable energy sources and its applications are significantly improved. One example of renewable energy is geothermal energy which can be used with the ground source heat pumps (GSHP) coupled with the ground heat exchangers (GHEs) buried underground. It has been published all over the world on geothermal energy applications [56] which manifested the ground source heat pump (GSHP) that was raised 2.15 times during 2005 to 2010. The compound annual rate is about 16.6% with an evidence of ground heat pump (GSHP) applications in 78 countries around the world.

The first construction of pile foundations as ground heat exchangers (GHE) were performed around 30 years ago in Austria [12] and known as energy piles. Currently, the utilization of energy piles is continuously growing, an example is in Austria where there are more than 100,000 of units installed [13]. Energy piles are cost effective which integrate two different important properties in one solution, the structural load-bearing and ground heat exchangers (GHE) i.e. thermal. In the meantime, the complexity of energy piles thermal

behavior makes it an important research topic.

The general scheme of the energy piles can be defined by the foundation plane which thermal interference between the closely located adjacent piles appear. The temperature of the soil and rock that surrounding energy piles increases with respect of the ground pile and circulating fluid thermal capacitance during the heat rejection process and will decrease during the heat extraction process. Generally, the balance of the operation of the energy pile is significant. Unbalanced operations, where the extracted heat is more than the injected, in some cases may result a significant decrease in long term energy performance. Thus, maintaining stable operation of energy piles is significant particularly in a long term. However, taking in consideration the seasonal-thermal storage may become feasible. In between the energy piles ground surface boundary and the building floor structure manifest additional thermal interference [26]. The performance of the energy piles can be significantly enhanced in cold climate areas, where the heat loss of building floor might heat up the ground over years and generated natural thermal storage effect. There are many factors with different variables that play significant roles such as thermal properties of the ground, grout, pipes, temperature boundary conditions, the pile's length, fluid, the distance between the piles, design, and optimal sizing of energy piles and/or ground source heat pump (GSHP). The factors that are listed above make the system with energy piles requires complex dynamic numerical modeling.

The objective of this section is to report and show various applications of energy piles and their potential as a renewable energy solution. Also, many different fundamental schemes of heat pump plants with energy piles will be presented and many different energy pile configuration types and their performance which are already studied. The following sections of this chapter will present and discuss available underground sizing and design techniques. As known, the operation principle of energy piles is similar to bore-holes [26] with known differences in boundary conditions. However, this study covers available scientific literature and design guideline materials related to energy piles topic, this literature be classified into four major categories which is presented in Tables 2.4 and 2.5.

2.2.1. Schematic of Plants with Energy Pile

Various schemes were conducted of geothermal plants. However, the most common one in energy pile applications can be shown in Figure 2.2 where the climate of indoor unit is totally ensured with heating. The methodology of this scheme can be explained in two different situations which are the secondary side demands either heat or cool. In the first case, the operation of a heat pump will heat up the heat carrier in the buffer tank. The operation to accommodate the desired temperature, whenever the tank's temperature drops below the arranged point value and the heat pump as well, built-in electrical heating coil or some other top-up heating begins its operation to heat up the tank volume to the desirable temperature value. In the second case, as shown in Figure 2.2 the circulating fluid in the energy piles loop is directly pointed to the "free cooling" heat exchanger. The heat exchanger, when combined secondary side, cools circulating fluid. However, from the Figure 2.2 there are three valves where they function as a reverse flow to the heat pump loop. Thus, the consequence of this processes is a reverse heat pump operation. According to this process, it can be said that the volume of the buffer tank can be alternately heated or cooled in such plant. If "free cooling" is incapable to accommodate most of the cooling demand, cooling circuit is appreciated in buildings. Nevertheless, it can be comprehended that such a plant might not be able to cool and heat the building simultaneously [27]. There is an example where this scheme is used in a two-stores residential building in Hokkaido, Japan [35].

The second scheme is shown in Figure 2.3 which is suitable for both cooling and heating conditions. Comparing this scheme with the previous one, we can see that the plant scheme considers an additional individual cooling machine and the design contains a cold buffer tank. Terminal E of the Zürich airport uses this type of scheme, which was constructed in 2003 and performs 306 of concrete energy piles as a ground heat exchanger (GHE) in plant design equipped with 5 U-pipes. This system is designed for accommodating both heating and cooling in the terminal [64]. According to the review is conducted by J. Fadejev *et. al* [27], the total capacity of the heat pump is 630 kW, which covers 85% of the heating demand. However, energy piles "free cooling" covers the cooling demand of the terminal.

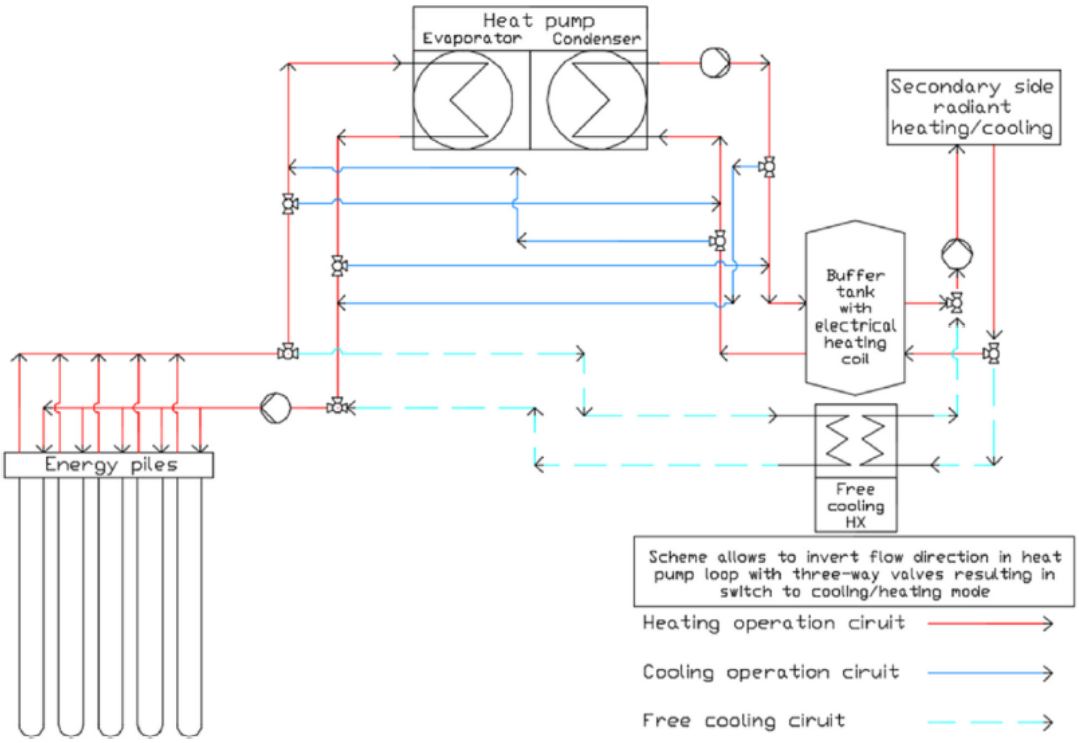

Figure 2.2. Hybrid heat pump plant with energy piles and "free cooling" option. Source: J. Fadejev *et. al* [27].

This project was done with the help of $PILESIM$ software, which utilizes finite difference method-based duct ground heat storage model (DST) [36]. The geometry of the piles is 900 - 1500 mm, 26.8 m, outer diameter and length of the piles, respectively. The production of the heat pump that is used is about 2210 MWh, which covered ca 73% of demand heat and the rest is covered with top-up district heating [64]. However, 620 MWh of cooling demand is completely covered by "free cooling" which was designed to satisfy its needs, which is about ca 53% cooling need annually.

As it was illustrated in earlier paragraphs, unbalance in both operation of extraction and re-injection might affect in the long-term performance of the geothermal energy piles operation. However, an ideal solution can be seen in Figure 2.4, where thermal storage can lead to stabilizing long-term operation of ground heat exchangers. This solution is highly recommended for structures that are located in cold places with low average annual outdoor temperature. In this kind of plant, there are many different resources of thermal storage such as solar storage (for example, solar collector), air source (for example, dry cooler or/and air handling unit exhaust air heat exchanger). There are examples using the terminology of Figure 2.4, but they were applied in ground source heat pump (GSHP) which was conducted by Reda [67]. A numerical study has been done on thermal solar application but not on energy piles.

There is another scheme where both seasonal warm and cold air source storages are presented. This plate solution can be shown in Figure 2.5. The operation of this plant during the summer and winter vary. For the operation in summer (cooling), the heat will be injected to the cold energy pile field, while the heat will be injected by the dry cooler into the warm energy pile field, and for the operation in winter (heating), the heat will be extracted by the heat pump from the warm energy pile field and the heat will be extracted by the dry cooler from the field of cold energy pile. An example of this scheme was conducted by Allaerts *et. al*, in Belgium [4] but not for energy piles.

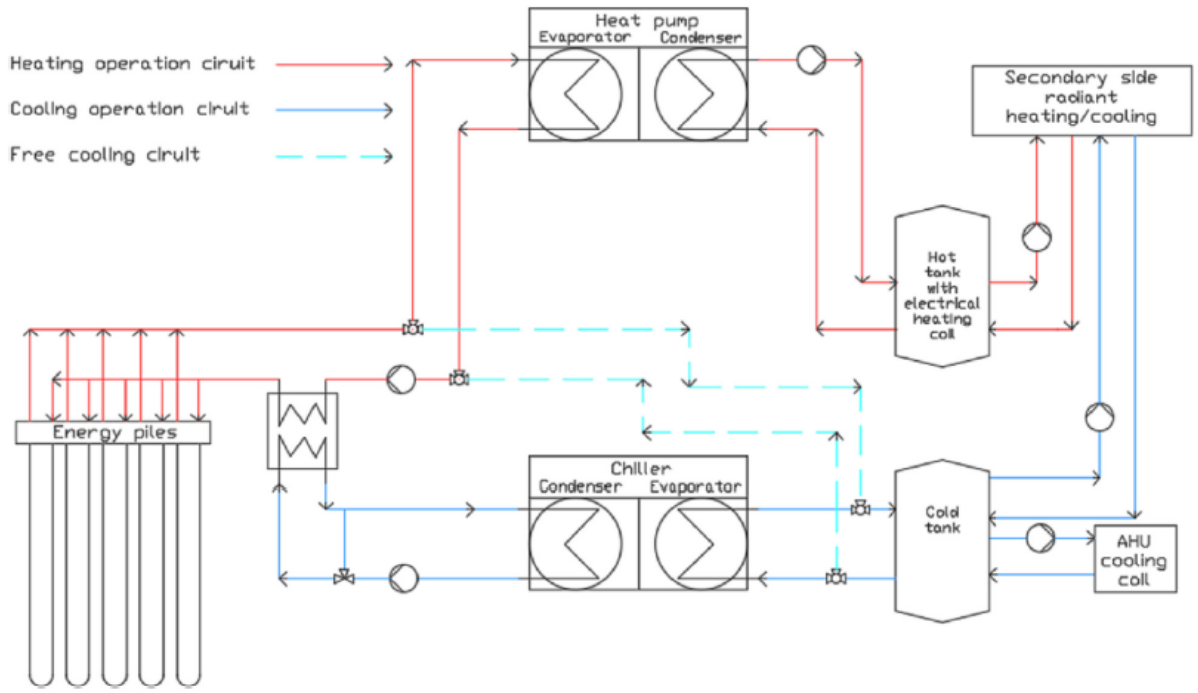

Figure 2.3. Hybrid heat pump plant with energy piles and "free cooling" option. Source: J. Fadejev *et. al* [27].

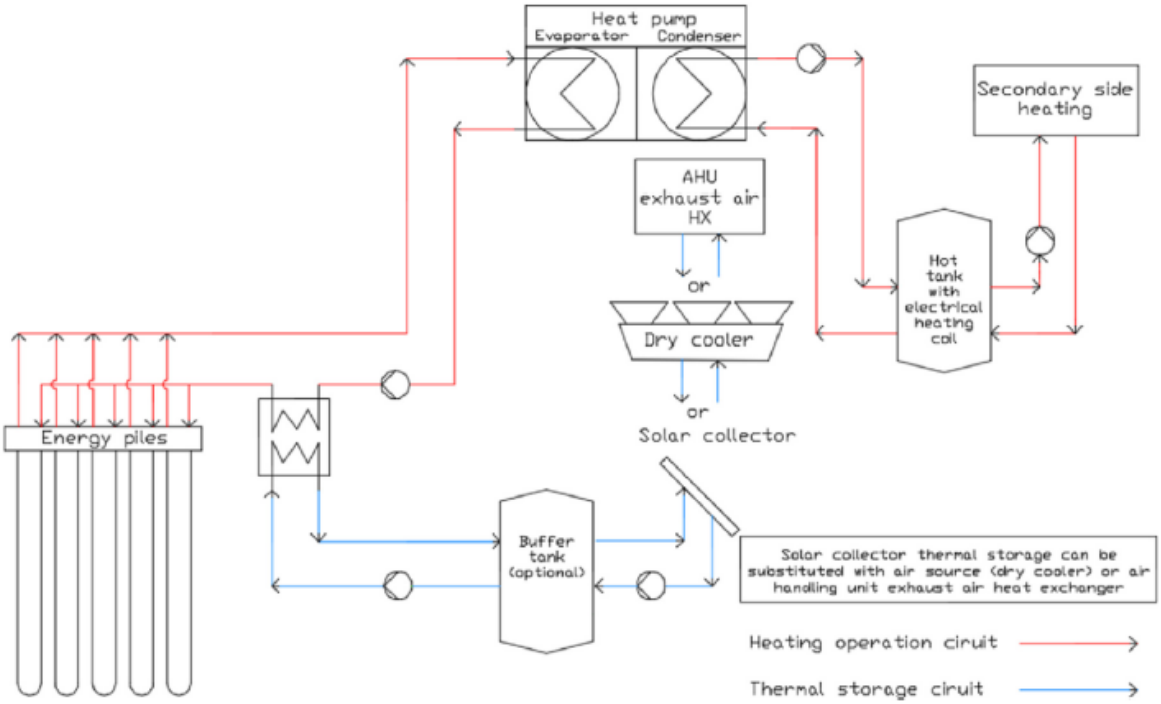

Figure 2.4. Heat pump plant with energy piles and solar/air source/AHU exhaust air HX thermal storage. Source: J. Fadejev *et. al* [27].

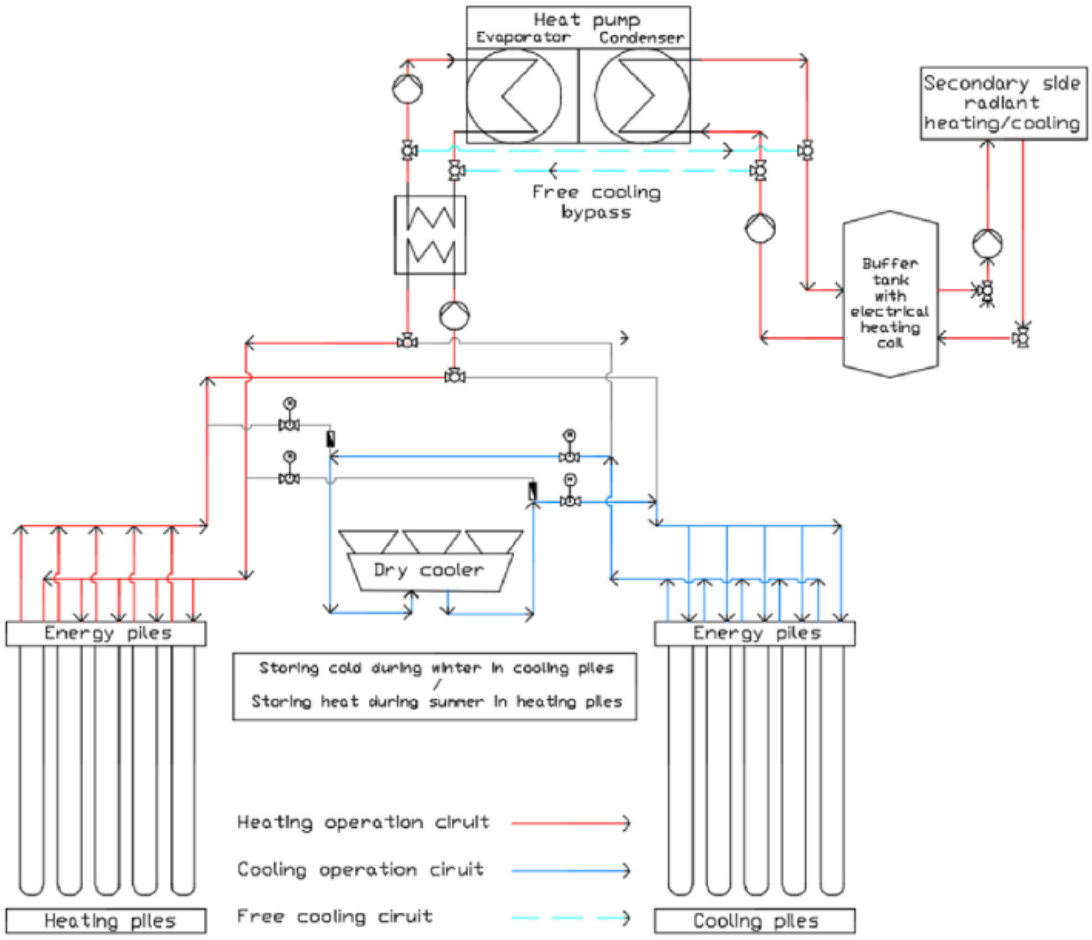

Figure 2.5. Heat pump plant with separated energy pile field for cooling and heating with air source thermal storage. Source: J. Fadejev *et. al* [27].

2.2.2. Configurations of Energy Piles

The configurations of energy piles depend on the the installation of heat exchange loops and the material of the piles as well. However, there are three common materials are utilized for piles such as prestressed high-strength concrete (PHC), cast in-situ concrete pile, and steel pile. The heat exchangers can be in many shapes such as single U-tube, double U-tubes, W-tube, and coils with known pitch and as indirect double pipes. There are also many shapes popular in research papers, but not in practice e.g. helix/spiral type exchanger. In contrast, U-loops with large diameters are more popular in practice. Some of the energy pile configuration can be seen in Figure 2.6. The soil thermal properties can be found on site by conducting the thermal response test (TRT) which helps get thermal conductivity, diffusivity of the soil, and the pile thermal resistance [85]. Thermal response test is also important in the estimation of the performance such as $/m$ capacity of different pile configurations. Furthermore, the test should be able to capture the short-term behavior of energy piles or at least carried out for a period to conquer the effect of thermal capacity of the energy pile.

2.2.3. Modeling of Energy Piles

Energy Piles Modeling is a new field of research compared to bore-hole modeling, but it can be said that, the operation of bore-holes is a bit similar to that of the energy piles. Also, huge variations can be seen in their operational conditions as heat exchangers. In general, comparing these two types of systems, the energy piles are shorter than bore-holes, i.e., bore-holes lengths are usually from 50 m extending up to 300 m. Because of the lack of the need to carry building load, bore-holes diameter is smaller compared to energy piles. Moreover, they are designed as a line source because their diameter is small compared to its length. As known, the length of energy piles is small and radially thicker due to their load bearing function compared to bore-holes. The structure of bore-holes are grout, pipe legs, and fluid, thermal capacitances are neglected [27].

The thermal behavior of piles on short-term application can be affected significantly by the thermal capacitance of the grout materials of the energy piles. However, the ground

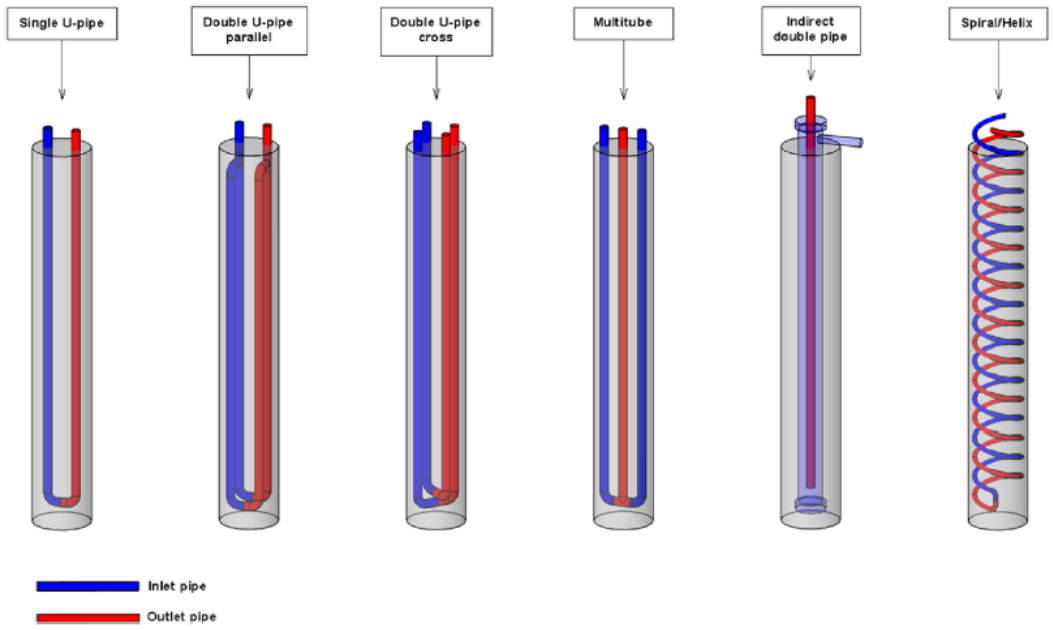

Figure 2.6. Energy pile configurations. Source: J. Fadejev *et. al* [27].

surface boundary of the energy piles could be modeled as adiabatic, and that will help to avoid accounting the effect of climate change over the year.

Energy piles can be modeled numerically by using various software. However, there are many advantages of numerical simulation such as quantifying the difference between 2D, 3D and quasi 3D models, more details about the modeling for those can be seen in these papers [8, 30, 86]. Detailed modeling might lead to a high computation time and modeling complexity, which cannot be applied for daily engineering applications.

2.2.4. Sizing and Designing of Energy Piles

There are no guidelines of the size and design of energy piles yet. However, design recommendations and installation guidelines are assigned to recommended standards or detailed numerical studies. Some standards contain simplified graphics, tables, data, and manuals to utilize more complex analytical sizing procedures. There are so many limitations in using standards which are suitable for small scale systems. The main purpose is to accommodate

heating with a design load of up to 45 kW. There are a lot of countries where these standard methods are used such as the Austria [71], Germany [79], Swiss [69], and UK [76] standards. There are so many examples of the standards limitations such as the actual sizing that can be performed only in the ranged length of 40-100 m for an individual bore-hole, German VDI 4640 [79]. Another example is UK standard MCS MIS 3005 demanded that the spacing between the adjacent bore-holes should to be at least 6 m [27].

Table 2.1. Installed geothermal generating capacities world-wide from 1995 to 2000 (from Huttrer, 2001), and in 2004.

Country	1995 (MWe)	2000 (MWe)	1995–2000 (increase in MWe)	%	2004
Australia	0.17	0.17	0	0	0.17
Austria	—	—	—	—	1.25
China	28.78	29.17	0.39	1.35	32
Costa Rica	55	142.5	87.5	159	162.5
El Salvador	105	161	56	53.3	162
Ethiopia	0	8.52	8.52	-	7
France(Guadeloupe)	4.2	4.2	0	0	15
Guatemala	0	33.4	33.4	–	29
Iceland	50	170	120	240	202
Indonesia	309.75	589.5	279.75	90.3	807
Italy	631.7	785	153.3	24.3	790.5
Japan	413.705	546.9	133.195	32.2	537
Kenya	45	45	0	0	127
Mexico	753	755	2	0.3	953
New Zealand	286	437	151	52.8	453
Nicaragua	70	70	0	0	77.5
Papua New Guinea	—	—	—	—	6
Philippines	1227	1909	682	55.8	1931
Portugal(Azores)	5	16	11	220	16
Russia	11	23	12	109	81.6
Thailand	0.3	0.3	0	0	0.3
Turkey	20.4	20.4	0	0	20.4
USA	2816.7	2228	588	n/a	2395
Total	683	7974	1141	16.7	8806.45

Table 2.2. Electric capacity from geothermal energy out of total electric capacity for some developing countries in 1998 (MWe).

Country	Total electric installed power	Geothermal electric installed power	% of the total power installed
Philippines	11601	1861	16.0
Nicaragua	614	70	11.4
El Salvador	996	105	10.5
Costa Rica	1474	115	7.8
Kenya	889	45	5.1
Indonesia	22867	589.5	2.6
Mexico	45615	755	1.7

Table 2.3. Non-electric uses of geothermal energy in the world (2000): installed thermal power (in MWt) and energy use (in TJ/yr)

Country	Power (MWt)	Energy (TJ/yr)	Country	Power (MWt)	Energy (TJ/yr)
Algeria	100	1586	Japan	1167.0	2693
Argentina	25.7	449	Jordan	153.3	1540
Armenia	1	15	Kenya	1.3	10
Australia	34.4	351	Korea	35.8	753
Austria	255.3	1609	Lithuania	21	599
Belgium	3.9	107	Macedonia	81.2	510
Bulgaria	107.2	1637	Mexico	164.2	3919
Canada	377.6	1023	Nepal	1.1	22
Caribbean Islands	0.1	1	Netherlands	10.8	57
Chile	0.4	7	New Zealand	307.9	7081
China	2282	37908	Norway	6.0	32
Colombia	13.3	266	Peru	2.4	49
Croatia	113.9	555	Philippines	1	25
Czech Republic	12.5	128	Poland	68.5	275
Denmark	7.4	75	Portugal	5.5	35
Egypt	1.0	15	Romania	152.4	2871
Finland	80.5	484	Russia	308.2	6144
France	326.0	4895	Serbia	80.0	2375
Georgia	250.0	6307	Slovak Republic	132.3	2118
Germany	397.0	1568	Slovenia	42.0	705
Greece	57.1	385	Sweden	377.0	4128
Guatemala	4.2	117	Switzerland	547.3	2386
Honduras	0.7	17	Thailand	0.7	15
Hungary	472.7	4086	Tunisia	23.1	201
Iceland	1469	20170	Turkey	820	15756
India	80.0	2517	United Kingdom	2.9	21
Indonesia	2.3	43	USA*	3 766.0	20302
Italy	325.8	3774	Yemen	1.0	15
TOTAL				15145	190699

During 2001 these figures increased to 4,200 MWt and 21,700 TJ/yr (Lund and Boyd, 2001). Source: Lund and Freeston, 2001 [55].

Table 2.4. List of studies conducted on topics related to energy piles design in chronological order [27]

Nr.	Reference	Fundamental schemes	Energy pile configurations	Modelling	Sizing & design
1	S.P. Kavanaugh and K. Rafferty [43]				✓
2	H. Brandl [11, 13]				✓
3	B. Sanner [72]	✓			
4	D. Pahud, M. Hubbuch [64]	✓			
5	Y. Hamada et al. [35]	✓	✓		
6	J. Gao et al. [28]		✓		
7	H. Yand et al [82]			✓	✓
8	T. Man et al. [57]			✓	
9	P. Hu et al. [38]			✓	
10	A. M. Jalaluddin et al. [60]		✓		
11	GSHPA [6]				✓
12	M. Li, A. C.L. Lai [49]			✓	
13	IGSHPA [40]				✓
14	A. Zarrella et al. [83]			✓	
15	W. Zhang et al. [86]			✓	
16	C. K. Lee and H.N. Lam [46]			✓	
17	O. Ghasemi-Fare and P. Basu [31]			✓	
18	S. Park et al. [65]		✓		
19	K. Allaerts et al. [4]	✓			
20	E. Hassani Nezhad Gashti et al. [30]			✓	

Table 2.5. List of studies conducted on topics related to energy piles design in chronological order [27]

Nr.	Reference	Fundamental schemes	Energy pile configurations	Modelling	Sizing & design
21	F. Dupray et al. [23]			✓	
22	F. Loveridge and W. Powrie [53]			✓	
23	T.V. Bandos et al. [8]			✓	
24	J. Fadejev and J. Kurnitski [25, 26]	✓		✓	✓
25	F. Loveridge and W. Powrie [52]			✓	
26	W. Zhang et al. [86]			✓	
27	M. Li, A. C.K. Lai [50]			✓	
28	E. Sailer et al. [71]				✓
29	D. Wang et al. [80]			✓	
30	A. Girard et al. [32]	✓			
31	A. Hesaraki et al. [37]	✓			✓
32	M. Aydin, A. Sisman [7]			✓	

Chapter 3

NUMERICAL SETUP AND METHODOLOGY

3.1. Introduction

The term energy piles refers coupling the structural pile foundations to heat exchangers roles where such foundations function to support the superstructure. Installed pipes where heat is carried by circulating fluid into them, takes advantage of the large thermal storage capabilities of the underground for cooling and heating purposes. It has been effectively used in individual buildings and infrastructure where these energy piles are connected to heat pumps is located in the structure above the ground. The function of heat pumps is to conveying the stored heat and energy input to the structure during heating season and the heat can be extracted from the conditioned spaces and injected into the soil, beside their energy input during the cooling season. However, utilization of the energy pile foundations skyrocketed recently due to their savings in the installation costs regarding their drilling process and hybrid character [10].

Identifying the performance of energy piles is different and depends on many factors such as pipe configurations, geometric design of the foundations, material properties of the foundation itself, surrounding media (i.e. soil/rock or a combination of both), and site layout. Moreover, the difference of restraint conditions and applied thermal loads have a huge effect on the geotechnical behavior of energy piles where these primary parts are connected and coupled through the energy piles over mechanical and thermal responses of these foundations.

Several studies were conducted in this field over the years where the thermal behavior of vertical ground coupled with heat exchangers, those studies were focused on many things such as the pipe configurations, the surrounding medias, and so on. Analytical [16, 84] and numerical [24, 59] models of different complexities were conducted in this field. Presently,

the thermal behavior analysis of energy piles has been performed in many researches worldwide [1, 2, 28]. However, modeling three dimensional asymmetric and time dependent characterization where the interaction between the pile and the surrounding soil, the fluid in the pipes, and the pipes themselves are often considered of this foundation in simplified ways which focus only on specific case studies and not coupled with the mechanics of the problem. Finally, the mechanical behavior difference of both the media surrounding the energy piles (i.e. soil and rock) and the foundation itself undergoing thermal loads has recently been performed in several numerical studies [62, 63, 68, 70, 77]. Moreover, the latest studies simplified the numerical modeling of the energy pile of complex thermal behavior by imposing the thermal power to the whole modeled foundations [29, 61]. These studies were conducted on homogeneous solids, without the inner pipes and the circulating fluid. From an energy engineering prospect, there were approximations for the physics governing the real problem, especially when considering models where the ground heat exchangers are connected to other building-plant subsystems within a global thermodynamic and energetic analysis [17]. Nevertheless, from a geotechnical and structural engineering prospect, this technique is on the side of safety, in particular, short-term because the whole foundation experiences the highest temperature variation, therefore, the maximum induced mechanical effects. The above simplifications could be not accurate in terms of performance predictions and non-optimal design choices.

Energy piles should be anatomized as capacity systems able of responding to any changing or phase shift in a difference of the boundary conditions. To be more specific, huge investigations should be performed on the thermal behavior of the foundation when considering the entire system (pipes pile-soil) as the heat exchange problem that is governed by the differences of the temperature between these components. Thus, the behavior of the coupled transient mechanical as aspects of the foundation should be anatomized as it governs the bearing response for the superstructure. However, in this study which focuses on the thermal and mechanical behavior of energy piles, a series of 3-D numerical sensitivity analyses comprising the considered aspects for a single full-scale energy pile is simulated and the results

are presented. This study was performed with reference to the foundation of the Kingdom tower located in Jeddah, Saudi Arabia. However, the pile foundation is simulated as energy piles and investigates the roles of pipe configurations and buried in different rock materials. This study was performed to focus on the influence between the thermal and mechanical behaviors of energy piles under transient conditions considering different technical solutions applicable to such foundations buried in rock materials.

In this study, the foundation is tested during its heating operation mode surrounded by rock which by considering the following design solutions:

1. The thermal response of the foundation in the short-term.
2. The time constants for approaching the steady state conditions of the heat exchange.
3. The heat transferred between the fluid in the pipes and the surrounding system are presented.
4. Geotechnical aspects related to the stress distribution in the pile.
5. The displacements fields characterizing the foundation depth are also considered.

3.2. Modeling of Energy Piles using 3-D Finite Element Method

3.2.1. The Simulated Site

The dimensions of the energy pile and the characteristics of the surrounding rock deposit considered in this study are those of an actual site located at Kingdom tower in Jeddah, KSA. The site includes a group of 270 piles installed below a heavily reinforced raft. The project of Kingdom tower's foundation were designed as traditional foundation piles not energy piles. This study considers only two types of the 270 piles with respect to a configuration denoted by a null head restraint and a null mechanical applied load on the top of the foundation [48]. The energy pile is characterized by a height H_{EP}= 105 and 45 m and a diameter D_{EP}= 1.5 m

(see Table 3.2). The pipes in the shallower 4 m are thermally insulated to limit the influence of the external climatic conditions on the heat exchange process. The characteristics of the rock deposit surrounding the piles are limestone and sandstone and the combination of both, as shown in Figure 3.1. The dimension of the geometric models and energy piles are listed in Table 3.2.

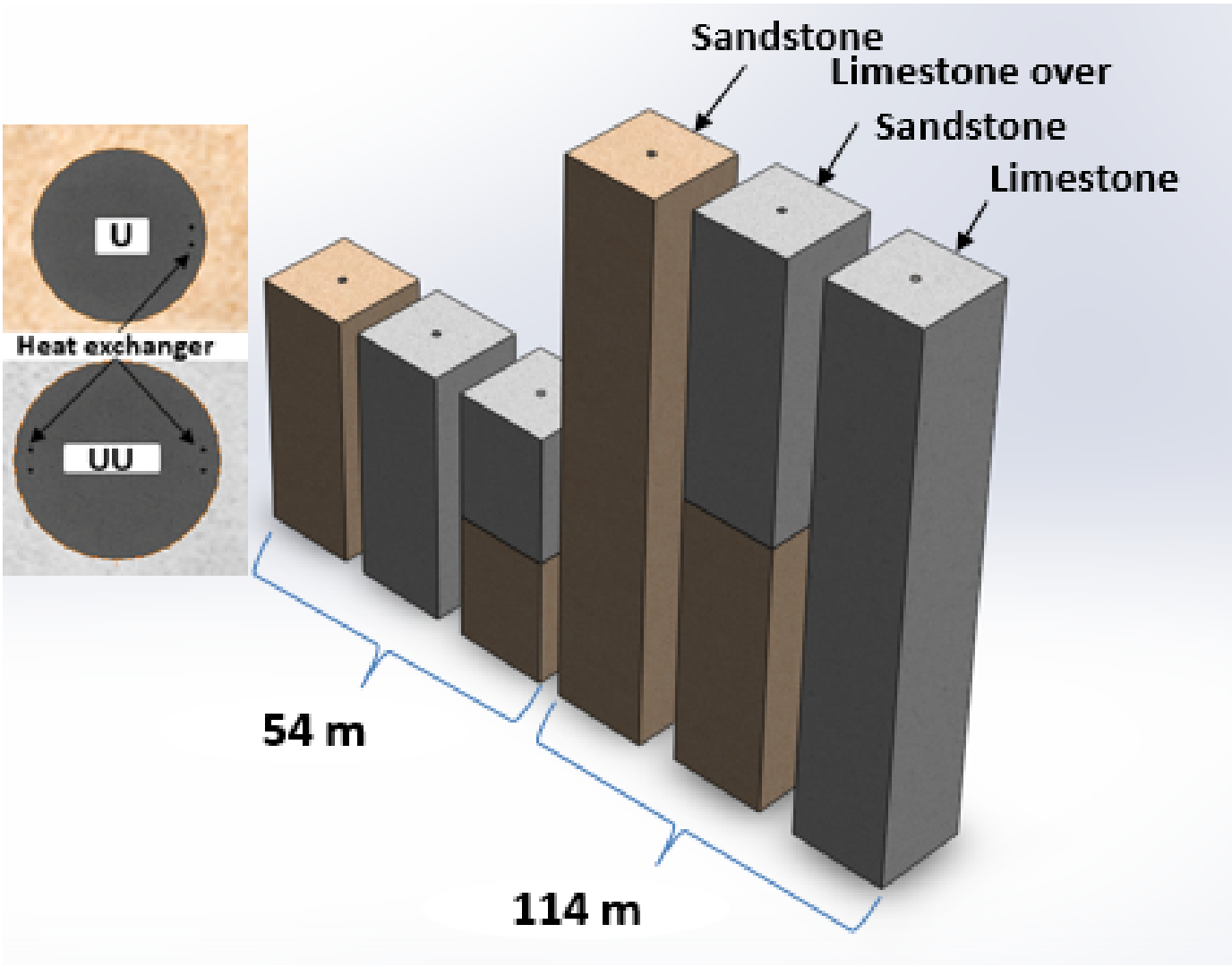

Figure 3.1. Typical rock stratigraphy surrounding the simulated energy foundation.

3.2.2. Simulated Geometry

In the presented study, there were 12 models, where six models were installed with single U-pipe and the remaining six models with double U-pipes. There were two different pile lengths considered herein as mentioned above in Section 3.2.1. Their dimensions and material properties again can be seen in Table 3.2 and Table 3.1, respectively. Cut sections which describe the details of the designed energy pile foundation and the installed pipe configurations for the two models can be seen in Figure 3.2 where the pile length is 105 m and Figure 3.3 for the pile with length equal to 45m. In both models, the first part of the model is the limestone type of rock and the second part is the sandstone.

3.2.3. Mathematical Formulation and Constitutive Models

To develop a quantitative illustration of the energy pile response which is considered to be buried in rock deposit under the mechanical and thermal loads, the next assumptions were performed:

- The rock layers were considered in these studies to be isotropic, fully saturated by water, and assumed to be purely conductive domains with equivalent thermo-physical properties given by the fluid and the solid phases.
- All the liquid and the solid phases were incompressible under isothermal conditions.
- The deformations and displacements of the solid skeleton were capable to be exhaustively illustrated through a linear kinematics approach which in quasi-static conditions i.e., negligible inertial effects.
- Drained conditions were satisfied during the analyzed loading processes.
- The behavior of all the rock and energy pile as linear thermo-elastic materials.

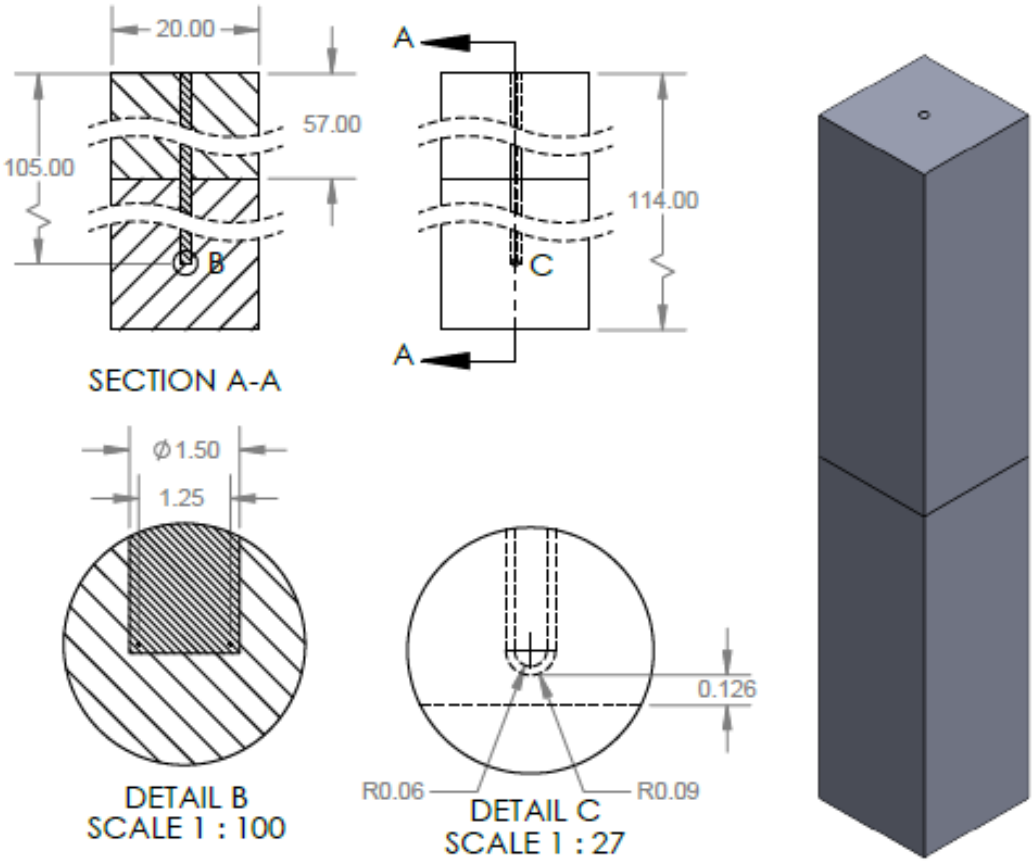

Figure 3.2. The 105 m pile and pipe configuration surrounded by rock.

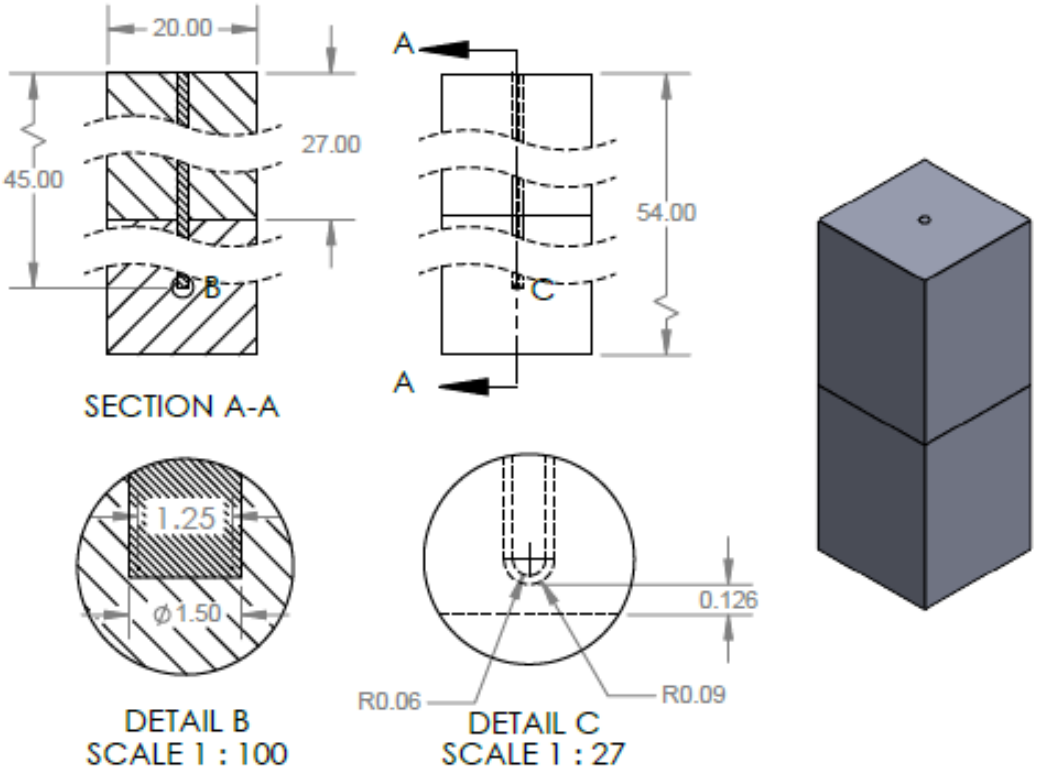

Figure 3.3. The 45 m pile and pipe configuration surrounded by rock.

Thus, under these assumptions, a coupled thermo-mechanical mathematical formulation was utilized in the following analyses.

The equilibrium equation [10] can be written as

$$\bigtriangledown \cdot \sigma_{ij} + \rho g_i = 0 \tag{3.1}$$

where:

$\bigtriangledown =$ denotes the divergence operator,

$\sigma_{ij} =$ denotes the stress tensor,

ρ = represents the bulk density of the porous material, which includes the density of water ρ_w and the density of the solid particles ρ_s, through the porosity (n); and (g_i) is the gravity vector.

The stress tensor can be expressed in incremental form as

$$d\sigma_{ij} = C_{ijkl}(d\varepsilon_{kl} + \beta_{kl} dT) \tag{3.2}$$

where:

$C_{ijkl} =$ is the stiffness tensor that contains the material parameters, i.e., the Young's modulus, E, and Poisson's ratio, υ;

$\varepsilon_{kl} =$ is the total strain tensor;

$\beta_{kl} =$ is a tensor that contains the linear thermal expansion coefficient of the material, α

T = is the temperature.

It was mentioned in the previous section that the concrete filling of the EP and the ground were assumed to be purely conductive media. With these assumptions, the energy conservation equation can be written as

$$\rho c \frac{\partial T}{\partial t} - \bigtriangledown \cdot (\lambda \bigtriangledown T) = 0 \tag{3.3}$$

where:

c = is the specific heat which includes water and solid components, c_w and c_s,

t = is time,

λ = is the thermal conductivity which includes water and solid components, (λ_w and λ_s),

$\bigtriangledown$ = represents the gradient operator.

In Equation 3.3, the first part is representing the transient component of the internal energy stored in the medium while the second part is representing the heat transferred by conduction (i.e., through Fourier's law). In the considered engineering application, the thermal properties of the fluid components were considered to be temperature dependent, whereas those of the solid components were considered to be temperature independent.

The energy conservation equation for the incompressible fluid flowing in the EP pipes can be shown as

$$\rho_f c_f A_p \frac{\partial T_{bulk,f}}{\partial t} + \rho_f c_f A_p u_f, i \cdot \bigtriangledown (T_{bulk,f}) = \bigtriangledown \cdot [A_p \lambda_f \bigtriangledown (T_{bulk,f})] + \dot{q_p} \tag{3.4}$$

where:

ρ_f = density of the fluid,

c_f = specific heat of the fluid,

A_p = pipe cross sectional area,

T_{bulk}, f= bulk temperature,

u_f, i = longitudinal velocity vector,

λ_f = thermal conductivity of the operative fluid are the density,

$\dot{q_p}$ = represents the heat flux per unit length exchanged through the pipe wall which is

given by

$$q_p^{\cdot} = UP_p(T_{ext} - T_{bulk,f}) \tag{3.5}$$

where:

U = an effective value of the pipe heat transfer coefficient,

Pp = $2\pi r_{int}$, the wetted perimeter of the cross section,

T_{ext} = the temperature at the outer side of the pipe.

The overall heat transfer coefficient which includes the internal film resistance and the wall resistance, can be obtained as follows:

$$U = 1\frac{1}{\frac{1}{h_{int}} + \frac{r_{int}}{\lambda_p} ln\left(\frac{r_{ext}}{r_{int}}\right)} \tag{3.6}$$

where:

h_{int} $= N_u\lambda_f/d_h$, The convective heat transfer coefficient inside the pipe,

λ_p = the thermal conductivity of the pipe,

r_{ext} and r_{int} = the external and internal radii,

d_h = $4A_p/P_p$ the hydraulic diameter,

N_u = Nusselt number.

For a given geometry, Nu is a function of the Reynolds, Re, and Prandtl, Pr, numbers, with

$$Nu_{turb} = \frac{(f_D/8)(Re - 1000)Pr}{1 + 12.7\sqrt{(f_D/8)}(pr^{2/3} - 1)} \tag{3.7}$$

$$f_D = \left[-1.8log_{10}\left(\frac{6.9}{Re}\right)\right]^{-1} \tag{3.8}$$

where:

$$RE = \frac{\rho v h}{\mu} \quad and \quad Pr = \frac{\mu_f c_f}{\lambda_f}$$

Equation 3.8 is the Gnielinski formula [33] for which turbulent flows. However, the friction factor, f_D, is assessed through the Haaland equation [34]. The equation is valid for very low relative roughness values which were used in this study.

3.2.4. 3-D Finite Element Model Features

In the presented studies, all the analyses were conducted utilizing the software COMSOL Multiphysics [18], which is a finite element simulation environment software. Also, it uses a high performance computing technique. In the this research, there were twelve models performed and studied by considering sensitivity analyses with respect to two different base-case models of a single energy pile equipped with a single U, and a double U type configuration of the pipes. The applied meshes of all models were user controlled. However, linear geometry shape in 3576 mesh elements were utilized to avoid inverted curved elements. Moreover, the number of degrees of freedom solved was 4,630,952 plus 61,065 internal degrees of freedom. The listed information in the above lines is for one model simulation which is an energy pile equipped with double U-pipes buried in limestone rock. However, the rest of the simulated models are in same range of mesh elements. In all the simulations, the maximum element size was 1.23 m and the minimum element size was 0.05 m. The maximum element growth rate was 1.34 and the curvature factor was 0.3. The resolution of the narrow regions is 1. Figure 3.4 describes the features of a typical model utilized in the study which is mainly focusing on the mesh used to characterize the pile that was equipped with different pipe configurations. In all conducted cases, the pipes were simulated with a linear entity in which the fluid was supposed to flow. Also, the distance of the pipes in all the designed models was 12.6 cm from the boundary of the foundation. However, the circulated fluid which flows inside of the pipes and their associated convective heat transfer was simulated by an equivalent solid [45] which possessed the same heat capacity per unit volume, i.e. specific heat multiplied by bulk density and thermal conductivity as the actual circulation fluid. The duration of the

considered studies were in rang of 17 - 50 minutes and were computed with high performance computing techniques.

3.2.5. Boundary and Initial Conditions

In term of boundary conditions, the restrictions were performed to both the horizontal and vertical displacements on the base of the mesh (pinned boundary see Figure 3.4) and a roller boundary was applied to the horizontal displacements on the sides. The initial stress state is caused by gravity in the rock and the pile was considered to be geostatic. Moreover, in terms of the thermal boundary conditions, the thermal boundary conditions allowed for the heat to flow through the vertical sides of the mesh and through the bottom of the mesh. The temperature of the rack was set to be 13.2 ^{o}C. The initial temperatures in the pipes, energy pile and rock were set at T_0= 13.2 ^{o}C, as an assumption of the average measured temperature at a site during winter [10]. Inside the installed pipes (high-density polyethylene tubes) where the fluid was circulating, the considered fluid in the base-case models was water. The inner diameter of the pipe was $\phi = 32 \ \ mm$ in all the simulated cases in this research and the nominal velocity of the fluid inside the pipes was u_f= 0.2 m/s. The temperature of the inflow fluid was set at $T_{in} = 5 \ ^{o}C$, again in all the implemented cases, also referred to the operation of the energy foundation in winter. At the shallower 4 m of the installed pipes, a thermal conductivity was imposed as $\lambda_p = 0 \ W/(m.K)$ to simulate the thermal insulation of the ducts near the ground surface. One shape of the simulated models, which contains the finite element mesh and the boundary conditions that were utilized in the simulations, can be shown in Figure 3.4.

3.2.6. Material Properties

The considered properties of the utilized rock deposit in these studies were defined based on previously published research papers (more details about the used material properties can be found in those researches papers [10, 47, 48, 78, 81]). For example, the rock thermal conductivity λ_r, the heat capacity c_r, density of rock ρ_r, porosity n, Poisson ratio ν, and elastic

modulus of the rocks E of both considered rock types. These values are also summarized in Table 3.1.

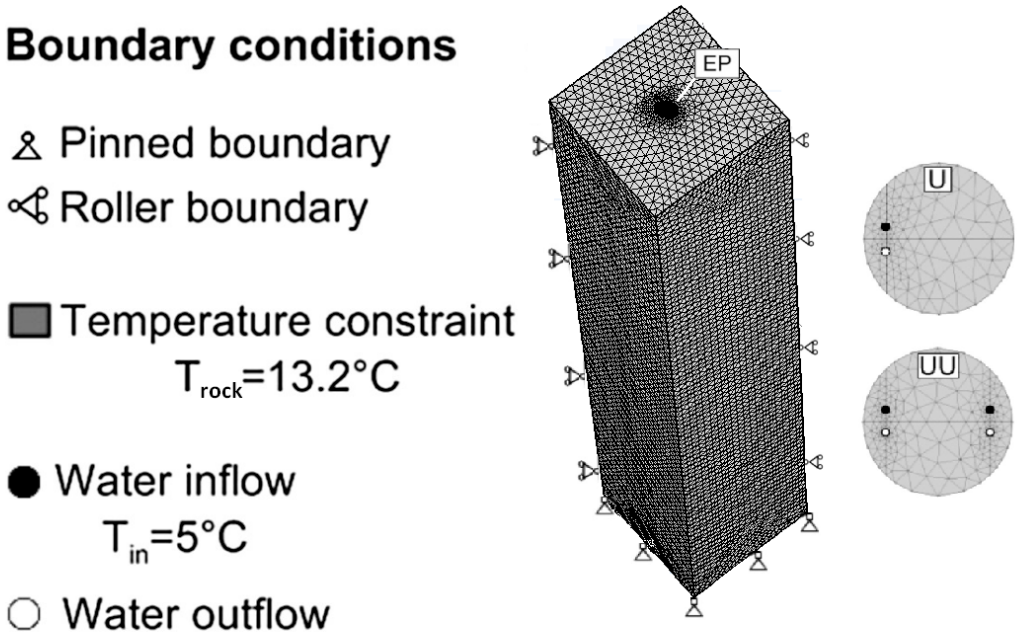

Figure 3.4. Finite element mesh and boundary conditions used in the simulations. EP: refers to energy pile.

3.3. Validation Results

3.3.1. 3-D Finite Element Modeling of an Energy Pile Embedded in Soil

This study was conducted by Niccolo Batini *et. al* in 2015 which was applied on various soil types for an experimental site located at the Swiss Federal Institute of Technology in Lausanne (EPFL), under the recently built Swiss Tech Convention Center [10]. However, the experimental site of the considered study includes a group of four energy piles. They were performed below a corner of a heavily reinforced raft which was used to support a water retention tank. The foundation of that water tank has eleven other conventional piles that

are not equipped as heat exchangers besides the four energy piles. Their study considered only one energy pile of the four energy piles with respect to a configuration denoted by a null head restraint and a null mechanical applied load on the top of the foundation. The energy pile is describes having a height $H_{EP} = 28$ m and a diameter, $D_{EP} = 0.90$ m. The shallower 4 m of the installed pipes were assumed to be thermally insulated which limit the effect of the climate change over the years. Figure 3.5 can define the soil types which were surrounding the energy pile and the dimension of their simulated model which are similar to those reported by Laloui *et. al* [44]. In their study, it has been assumed that the ground water table at the test site is at the top of the deposit. The top soil profile consists of alluvial soil for a depth of 7.7 m. Below this layer, a sandy gravelly moraine layer is located at the depth between 7.7 and 15.7 m. Followed by a stiffer thin layer of bottom moraine located at a depth between 15.7 and 19.2 m. Ultimately, a molasse layer is available below the bottom moraine layer [10].

3.3.2. The Features of the 3-D Finite Element Model

This study was conducted by the help of the software COMSOL Multiphysics [18]. This software is a finite element simulation environment and the model was designed by using the software SOLID-WORKS. Also, it used high performance computing techniques. The analysis was developed with respect to the model of a single energy pile foundation with a single U-shaped type configuration of the pipes. The mesh was set to be physical-controlled (Extra-fine) mesh consists of 248330 domain elements, 28337 boundary elements, and 2358 edge elements. Moreover, it used a linear geometry shape in 1120 mesh elements to avoid inverted curved elements. However, the number of degree of freedom solved was 1,646,082 plus 80631 internal degrees of freedom. The simulated pipe was developed with linear entity in which the fluid was supposed to flow and the there was a distance of 12.6 m where the center of the pipe was placed from the boundary of the foundation. The circulated fluid inside the simulated pipe and the associated convective heat transfer was simulated by an equivalent solid [45], which possessed the same heat capacity per unit volume such as specific

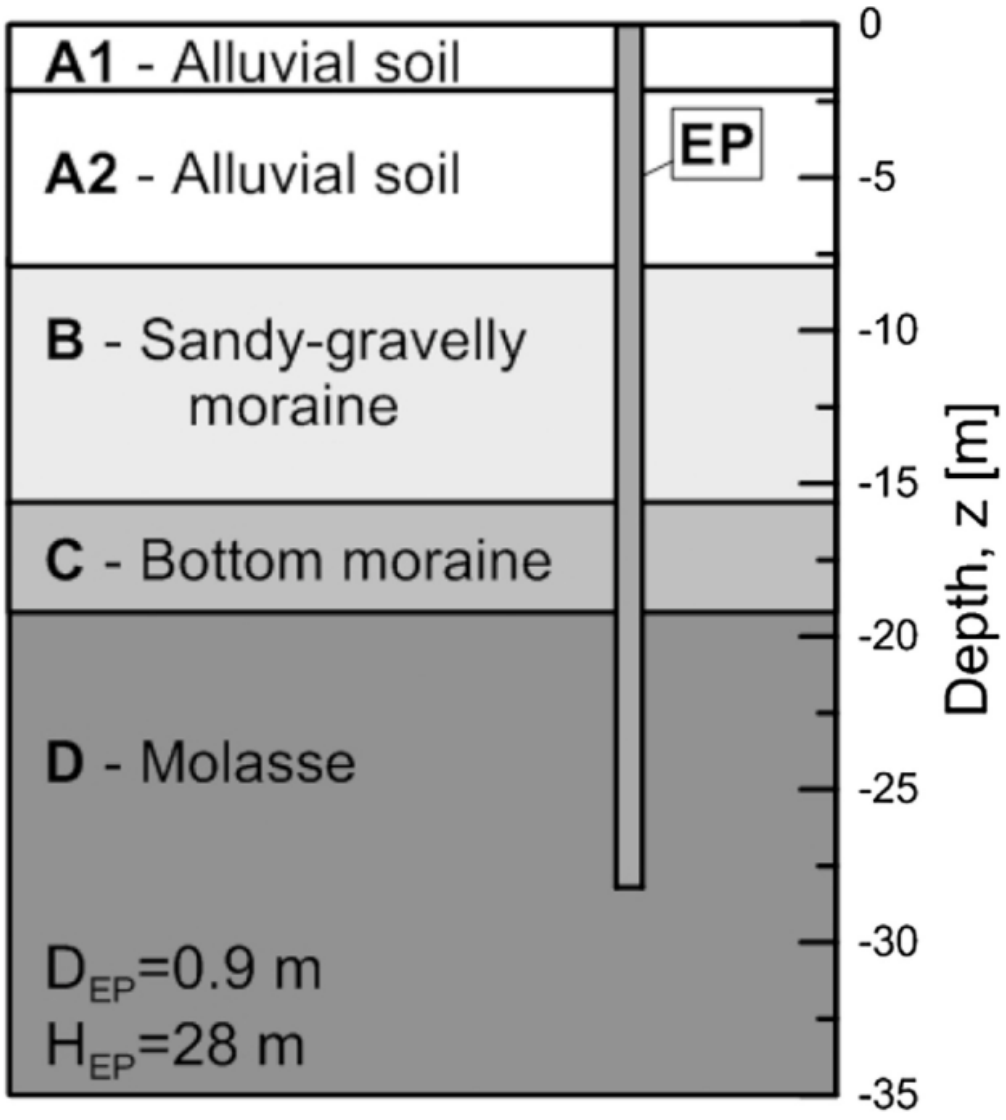

Figure 3.5. Typical soil stratigraphy surrounding the Swiss Tech Convention Centre energy foundation. EP: refers to energy pile. Source: Batini *et. al* [10].

heat multiplied by bulk density and thermal conductivity as the actual circulation fluid [10]. The duration time of these studies were in range of 14 - 17 minutes by using high performance computing techniques.

3.3.3. Boundary and Initial Conditions

On the base of the mesh, restrictions were performed in both the vertical and horizontal displacements and to the horizontal sides which can be seen in Figure 3.6. However, in term of the thermal boundary conditions, the heat flows either through the vertical sides of the mesh or through the bottom of the mesh. The temperature of the soil was set to be T_{soil}= 13.2 ^oC . The initial temperatures in the pipes, energy pile and rock were set at T_0= 13.2 ^oC, which is the average measured temperature at the considered site during winter [10]. It has been considered that the initial stress state caused by the gravity in the pile and the soil to be geostatic [10]. In the considered pipes (i.e. high-density polyethylene tubes) the circulated fluid was assumed to be water and its nominal velocity was u_f= 0.2 m/s. In the studied case, the assumed diameter of the pipes was set to be $\phi = 32 \ \ mm$ and the its temperature was $T_{in} = 5\ ^oC$, more information can be seen in Figure 3.6. The first 4 m of the pipe were thermally insulated to simulate the thermal insulation of the ducts near the ground surface. All the above listed values for the boundary and initial conditions were assumed to be the same as the study were conducted by Batini *et. al* [10] in 2015.

3.3.4. Material Properties of the Model

The material properties of the soil deposit, energy pile and pipes properties can be seen in Table 3.3.

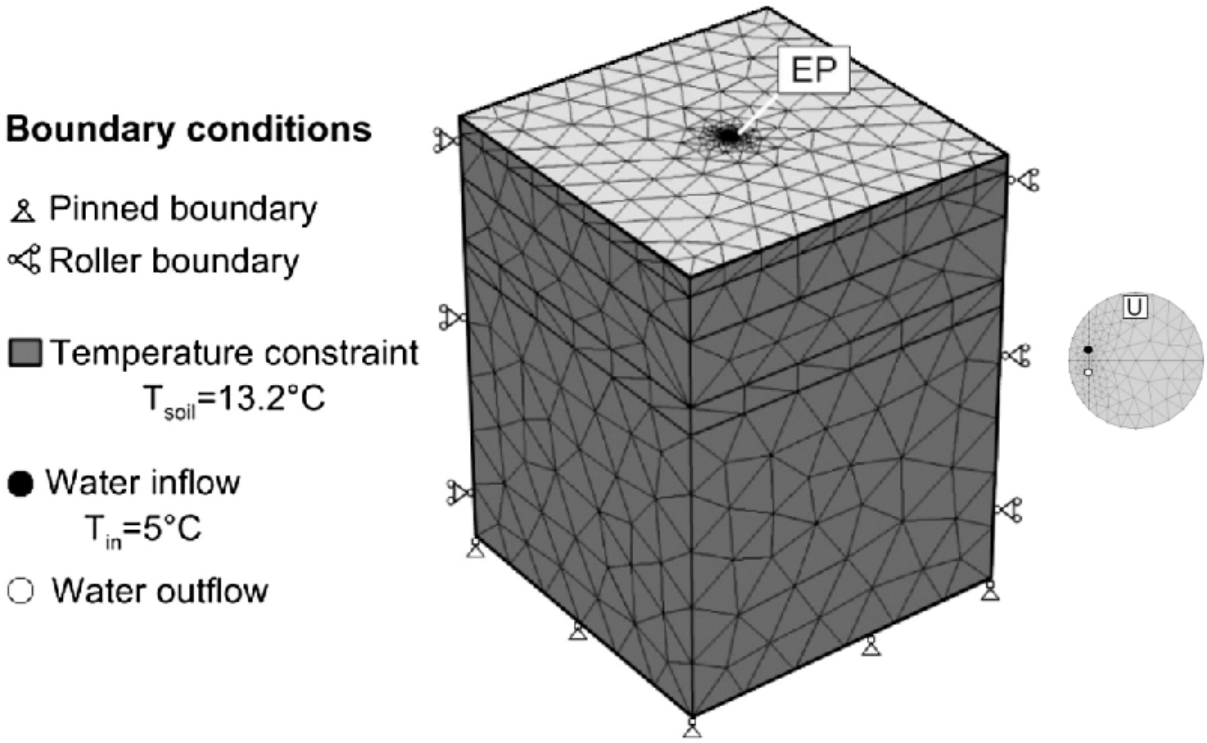

Figure 3.6. Finite element mesh and boundary conditions used in the simulations. EP: refers to energy pile. Source: Batini *et. al* [10].

Table 3.3. Material properties of the soil deposit, energy pile, and pipes. Source: Batini *et. al* [10]

	E $[MPa]$	ν $[-]$	n $[-]$	ρ_s $[kg/m3]$	c_s $[J/(kgK)]$	λ_s $[W/(mK)]$	α $[1/K]$
Soil layer							
A1	190	0.22	0.1	2769	880	1.8	0.33×10^{-5}
A2	190	0.22	0.1	2769	880	1.8	0.33×10^{-5}
B	84	0.4	0.35	2735	890	1.8	0.33×10^{-4}
C	90	0.4	0.3	2740	890	1.8	0.33×10^{-4}
D	3000	0.2	0.1	2167	923	1.11	0.33×10^{-6}
Energy pile pipes							
Concrete	1926	14.8	129.180	1911.86	99.40		
HDPE	-	-	-	-	-	0.42	-

3.3.5. The Result of the Model due to the Influence of a Single U-Shaped Configuration of the Pipes

The results of the thermal mechanical behavior of energy pile equipped with a single U-shaped pipe were investigated. However, Figure 3.7 describes the axial distribution of the temperature with the energy pile equipped with single U-shaped pipe configuration. It can be clearly noticed that in the first 4 meters of pile foundation there is no remarkable temperature characterization in that region. The pile at that region was thermally insulated. After 15 days of the operation, at the center of the pile where the pipe was equipped, the pile underwent an average cooling of ΔT=T-T_0= -3.6 ^oC. From Figure 3.7, it be observed that a little more cooling occurs at the last part of the pile where the molasse layer is located which due to its lower thermal conductivity which exhibited and induced a lower heat exchange with the foundation. Also, it has been noticed that the distribution of the temperature at the axial depth of the foundation did not significant vary in the simulation operation from 7 and 15 days, which means that the thermal conditions inside the pile were almost close to the steady state condition after a week of operation.

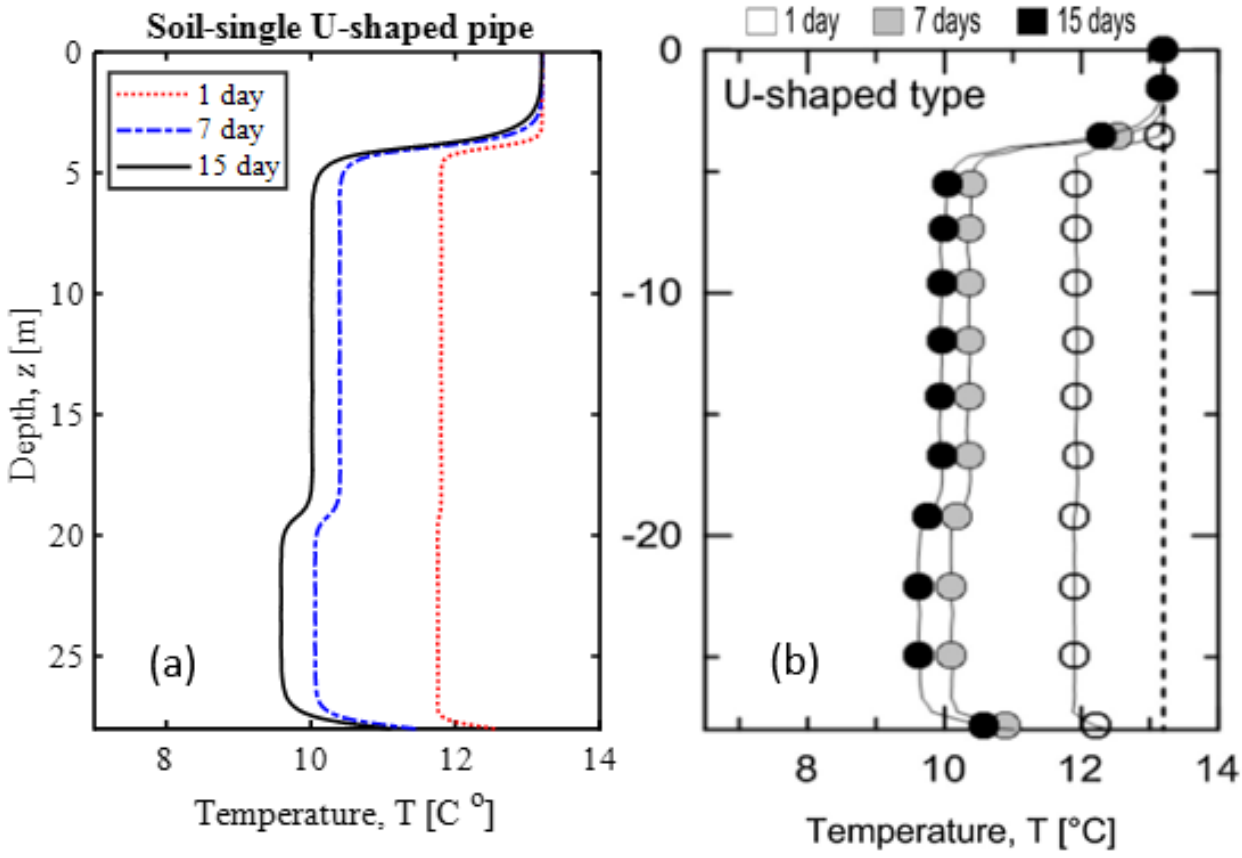

Figure 3.7. Comparison between (a) obtained and (b) published results for the axial temperature distributions for the single U-shaped pipe configuration.

Figure 3.8 describes the axial distributions of stress induced by the above-described temperature variations (which is in Figure 3.7). The maximum vertical stress was $\sigma_{v,th} = 900$ kPa, which was recorded along the axial depth of the energy pile foundation, exactly where the molasse layer is located. It can be noticed that these findings are consistent with the above-mentioned data because the pipe configuration that led to the maximum negative temperature variations inside the pile is due to the lower thermal conductivity of that region of the pile which induced the maximum thermal stress in the energy pile foundation.

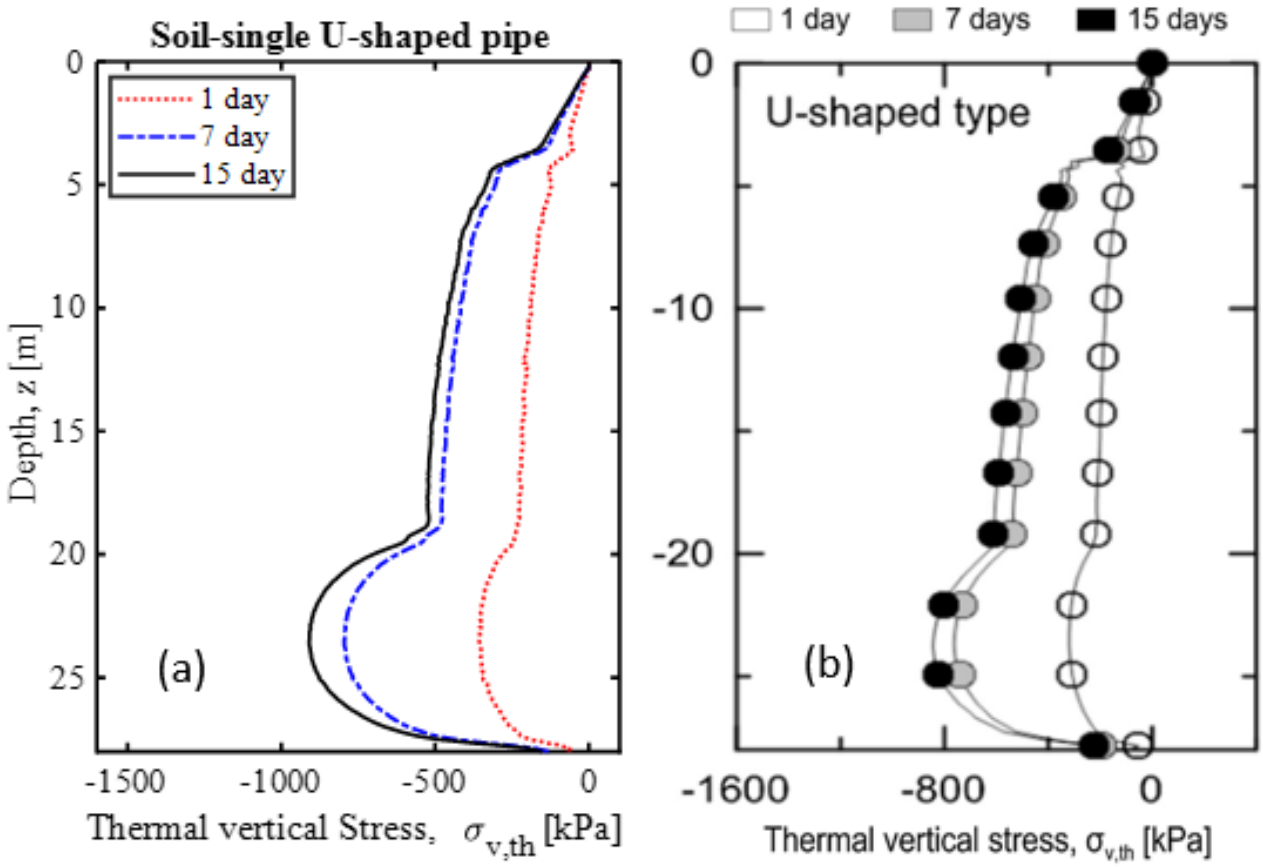

Figure 3.8. Comparison between (a) obtained and (b) published results for the axial distributions of the thermal vertical stresses for the single U-shaped pipe configuration.

The axial distribution of the vertical displacements for the energy pile are shown in Figure 3.9, which is consistent with the distributions of the observed temperature and stress. The maximum displacement of the energy pile with the equipped single U-shaped pipe was dz_{th} = 0.28 mm. The thermal displacement was zero at the bottom of the pile which represents the null point which was the same in the studies were conducted by Batini *et. al* [10] and Gashti *et. al* [29].

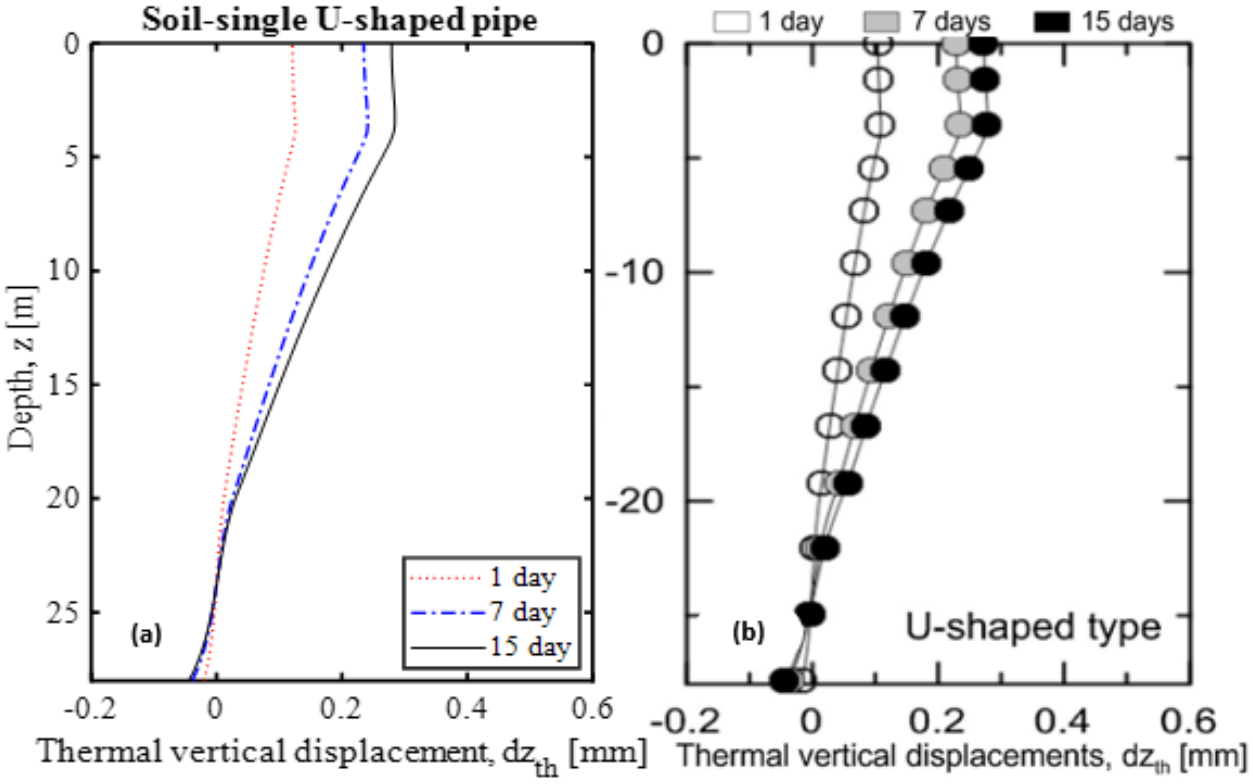

Figure 3.9. Comparison between (a) obtained and (b) published results for the axial distributions of the thermal vertical displacements for the single U-shaped pipe configuration.

Table 3.1. Material properties of the rock deposit, energy pile, and pipes.

Material Properties	E [MPa]	ν [-]	n [-]	ρ_s [kg/m3]	c_s [J/(kg K)]	λ_s [W/(m K)]	α [1/K]
Rock type							
Limestone	500	0.35		1836	890	3.44	2.4e-5
Sandstone	1000	0.3		2039	1400	3	3e-5
Energy pile and pipes							
Concrete	28000	0.25	0.1	2500	837	1.628	1e-5
HDPE						0.42	

Table 3.2. Geometric Design and Pile Dimension.

Model Geometry	Length [m]	Width[m]	Height [m]	Diameter Ø [m]
Limestone (A)	20	20	54	
Limestone (B)	20	20	114	
Sandstone and Limestone (A)	20	20	54	
Sandstone and Limestone (B)	20	20	114	
Sandstone (A	20	20	54	
Sandstone (B))	20	20	114	
Pile (A)			45	1.5
Pile (B)			105	1.5

Chapter 4

RESULTS AND DISCUSSIONS

4.1. Thermo-Mechanical Sensitivity of the Energy Piles to the Different Technical Solutions

In this section, sensitive results will be presented. The findings of the considered utilization techniques of different numerical sensitivity analyses were performed on various pipe configurations inside of the single energy pile that were conducted through 3-D transient finite element simulations, occurred over 15 days in winter. This period was proven to be adequate to reach the steady-state within the energy pile (EP) domain. Thus, the enthalpy changes of the fluid from the fluid entrance gate (inlet) to the exiting section (outlet) of the pipes corresponded to the thermal power exchanged at the energy pile outer surface which is the one in contact with the rock. However, in such situations, the effect of the heat capacity was negligible, and the behavior of the energy pile was typically like a heat exchanger which was described by an equivalent thermal resistance between the ducts and the rock. It has been utilized as the classical effectiveness method for heat exchangers [41] to compare and assess the process of heat transfer among the different energy pile (EP) configurations. However, the heat exchanger effectiveness ϵ_{he} can be defined as

$$\epsilon_{he} = \frac{T_{out} - T_{in}}{T_{r-p} - T_{in}} \tag{4.1}$$

where, ϵ_{he} represents the heat exchanger effectiveness, T_{r-p} is the average temperature at the rock-pile interface. However, it was considered compressive stresses and strains to be positive as were the downward displacements (settlements).

4.1.1. Influence of the Pipe Configurations and Rock Materials

An investigation was conducted on the thermal-mechanical behavior of the energy pile which were equipped with a single U-pipe and double U-pipe shapes. In both considered pipe configurations, the rock materials are limestone, sandstone, and combination of 50/50 limestone and sandstone.

The presented findings will discuss the three considered rock materials. There were two different pile dimensions which are domain (A) and domain (B). The results of domain (A) will be presented and discussed first and then for domain (B). More information about their dimensions and shapes can be seen in Table 3.2 and Figure 3.1.

4.1.1.1. Distributions of the Temperature for Each Type of Pipe Configuration and Rock Materials for Domain (A)

Figure 4.1 shows the axial distributions of the temperature for each type of configuration. As can be noticed, no remarkable temperature variation characterized the shallower 4 m of the foundation because the pipes in this region were thermally insulated. After 15 days, the center of the foundation equipped with a single U, and double U-shaped pipe configurations underwent an average cooling of ΔT=T-T_0=-2, -3.7 ^oC, respectively. It has been observed that the double U-shaped geometry of pipes experience the highest temperature variation because it involved the highest quantity of cold water in the heat exchange process.

A more pronounced cooling was observed on part of the pile in the model that consists of limestone and sandstone together. Even though the limestone has a slightly higher thermal conductivity than sandstone (3.44 compared to 3 $W/m \cdot K$), the lower heat capacity of limestone resulted in lower heat transfer to the pile from the surrounding rock material. Therefore, the pile experienced less heating from the limestone and more cooling from the nearby cold pipes. This fact caused a reduction in the heat exchange with the foundation, which is also observed when comparing the temperatures of the piles surrounded by limestone to those surrounded by sandstone.

The distribution of the temperature along the axial depth of the foundation did not remarkably change in most of the simulated cases between 7 and 15 days, which means that the system approaches steady state thermal conditions after the first week of operation.

4.1.1.2. Distributions of the Stress for Each Type of Pipe Configuration and Rock Materials for Domain (A)

Figure 4.2 describes the axial distributions of stress which are induced by the above described temperature variations (Figure 4.1). The maximum values of the stresses are $\sigma_{v,th}$ = -1000, 1900 kPa, observed along the axial depths of the foundation for the single U, double U-shaped pipe configurations, respectively. The initial stress distribution due to the load of the foundation body is subtracted. This thermal stress occurred in the combination of the limestone and sandstone types of rocks where the single U, double U-shaped pipe configurations were installed. However, the maximum values of the limestone-embedded system are $\sigma_{v,th}$ = 785, 1475 kPa, noticed along the axial depths of the foundation for the single U, double U-shaped pipe configurations, respectively. Moreover, for the sandstone, the maximum value of the thermal stresses were $\sigma_{v,th}$ = 817, 1618 kPa at the axial depths of the foundation for the single U, double U-shaped pipe configurations, respectively. However, the thermal stress results were consistent with the previously observed data because the configurations of the pipes pointed to the greatest negative temperature variations inside the pile (the configurations for which the greatest stresses were observed from the foundation thermal contractions). The magnitude of the stress which were induced by the temperature variation in the energy pile equipped with the single U-shaped pipe configuration was close to the one characterizing the results obtained by Batini *et. al* [10] and Gashti *et. al* [29] for which a single energy pile that was studied in winter conditions with the same type of pipe configurations.

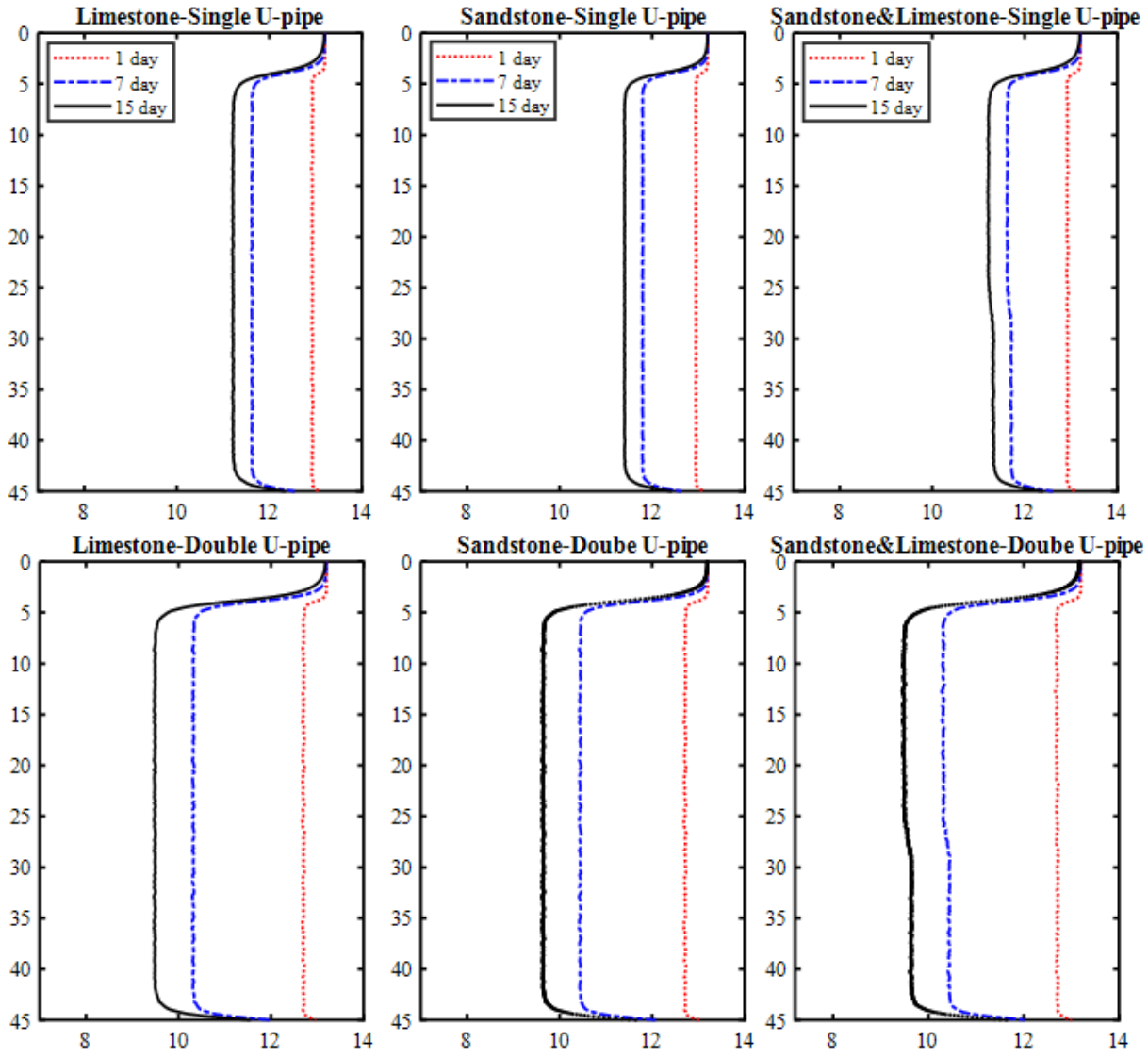

Figure 4.1. Axial temperature distributions for the U pipe (Top) and the doube-U pipe (Bottom) configurations embedded in limestone (Left), sandstone (Center), and a combination of both (Right) rock materials for domain (A).

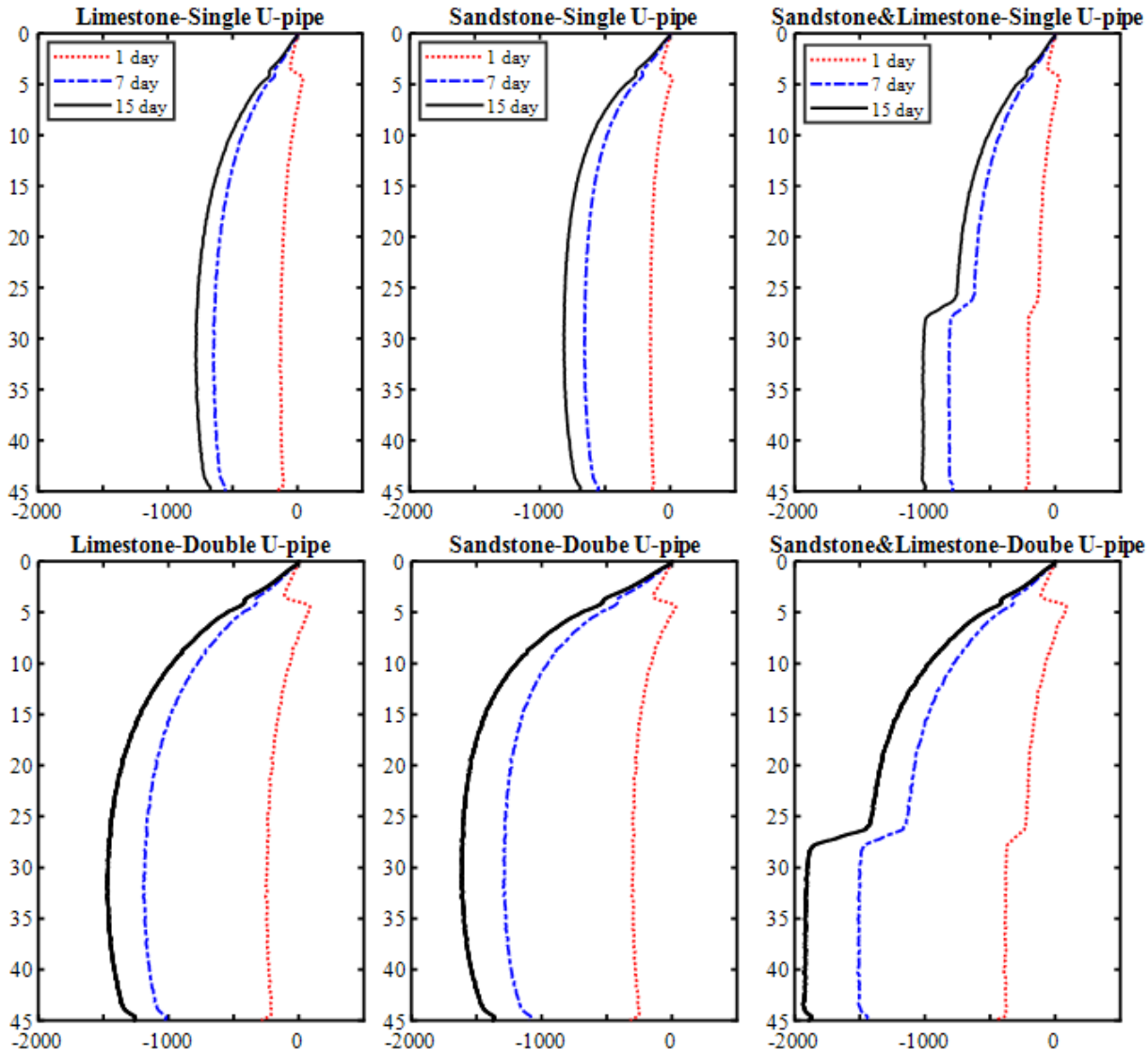

Figure 4.2. Axial distributions of the thermal vertical stresses for the U pipe (Top) and the doube-U pipe (Bottom) configurations embedded in limestone (Left), sandstone (Center), and a combination of both (Right) rock materials for domain (A).

4.1.1.3. Distributions of the Displacement for Each Type of Pipe Configuration and Rock Materials for Domain (A)

The axial distribution of the vertical displacement is presented in Figure 4.3. For all considered configurations, the displacements were consistent with the distributions of the temperature and stress profile. In most of the simulated cases, the results were close to the one was obtained by Batini *et. al* [10] for the pile foundation equipped with a single U-pipe and double U-pipe configurations. However, in term of displacement, the maximum effect of the cold flow within the tubes is observed for the pile foundation equipped with double U-pipe configuration. In contrast, the minimum effect is observed for the pile foundation equipped with a single U-pipe configuration. The maximum pile settlements $dz_{th} = 0.49$, 0.9 mm are noticed when the pile foundation equipped with a single U-pipe and double U-pipe configurations, respectively, buried in limestone type of rock. Moreover, the maximum displacement of the pipe foundation buried in sandstone are $dz_{th} = 0.31$ and 0.6 mm for the same pipe configurations, respectively, and for the maximum displacement of the combination of both limestone and sandstone are $dz_{th} = 0.33$ and 0.63 mm observed when the energy pile foundation is equipped with the single U, double U, respectively. It has been observed that the null point, which describes the plane where zero thermally induced displacement happens in the foundation, in all the simulated cases is in the bottom of the energy pile, which are very similar to the results obtained by Batini *et. al* [10] and Gashti *et. al* [29].

4.1.1.4. Distributions of the Temperature for Each Type of Pipe Configuration and Rock Materials for Domain (B)

The energy pile studied in Domain (B) has an extended length of 105 m. The axial temperature distributions for the different pipe configurations are shown in Figure 4.4. The first 4 m of the pipes are thermally insulated, similar to the conditions applied for domain (A), which resulted in no remarkable temperature variation for the shallowest 4 m of the foundation. Also, the center of the pile foundation equipped with single U and double U-shaped pipe configurations, after 15 days, underwent an average cooling of ΔT=T-T_0=-1.9,

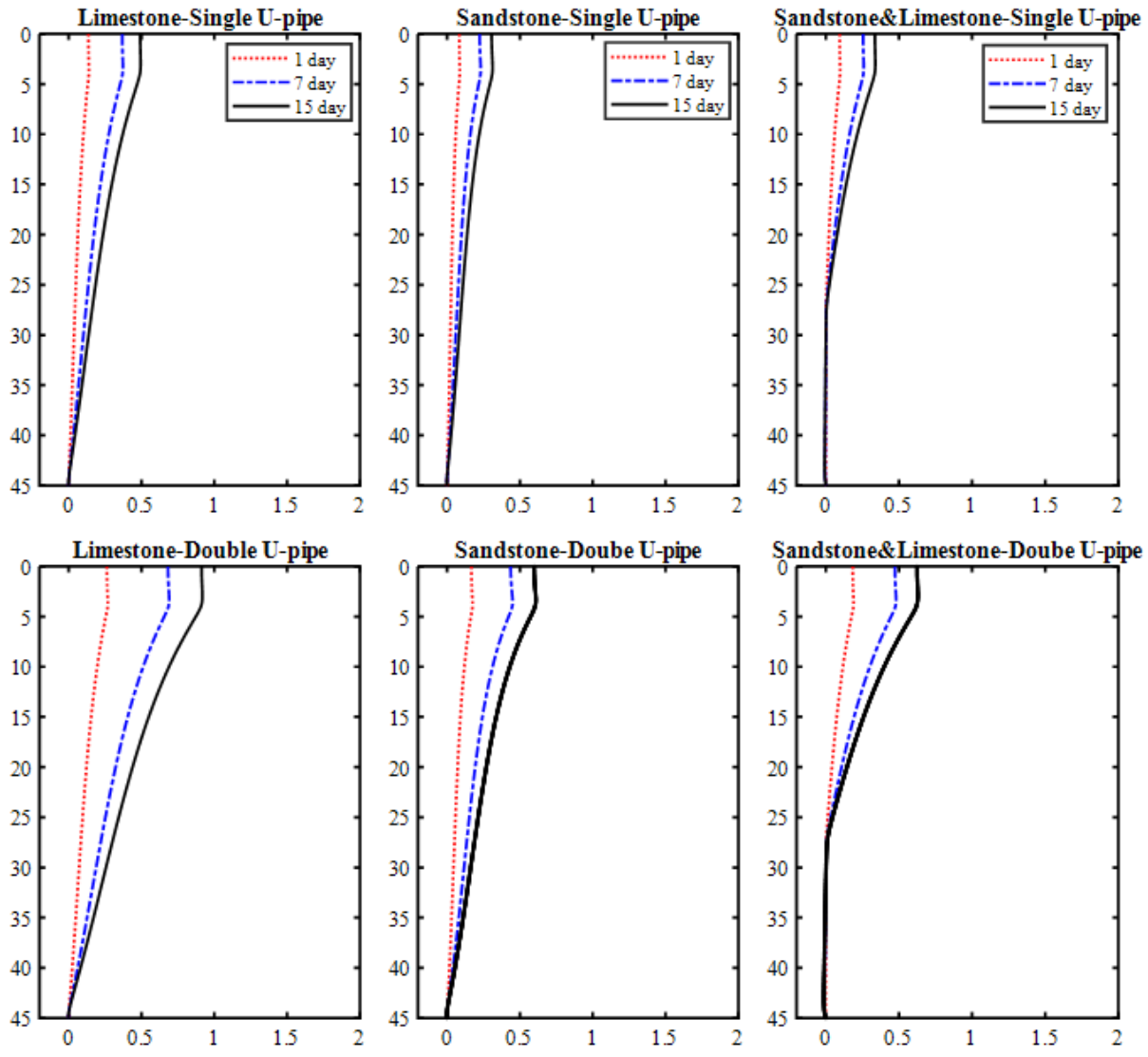

Figure 4.3. Axial distributions of the thermal vertical displacements for the U pipe (Top) and the doube-U pipe (Bottom) configurations embedded in limestone (Left), sandstone (Center), and a combination of both (Right) rock materials for domain (A).

-3.5 ^{o}C, respectively. Again, the greatest variation of temperature was reached with the double U-shaped geometry of pipes because it involved the highest quantity of cold water in the heat exchange process, for similar reasons to those mentioned earlier for domain (A).

It has been observed that limestone experienced more cooling of the first part of the pile, which is caused by a higher cooling from the pipes, and less heating from the foundation. Even with the higher thermal conductivity of the limestone layer, the low heat capacity of the surrounding material caused its temperature to drop and the transferred heat to the pile to be less than that observed in the case of sandstone.

Furthermore, it has been illustrated that in domain (B), the rate of temperature change in the axial energy pile depth was reduced for all the considered cases between day 7 and 15 of operation. This shows that after day 7, the thermal conditions inside the pile are already close to steady state, which show similar behavior to the studied models in domain (A) and to the result obtained by Batini *et. al* [10] were observed.

4.1.1.5. Distributions of the Stress for Each Type of Configuration and Rock Materials for Domain (B)

The axial distributions of the stress for each type of configuration and rock materials can be seen in Figure 4.5. The maximum observed values of the stresses are $\sigma_{v,th}$ = -1055, -1976 kPa, developed along the axial depths of the foundation for the single U, double U-shaped pipe configurations, respectively. However, the distribution of the initial stress generated by the load of the foundation body is subtracted. The above provided values of the maximum vertical thermal stresses recorded in the model with the combination of the limestone and sandstone rock where the single U, double U-shaped pipe configurations were installed. Moreover, the maximum values of the limestone of $\sigma_{v,th}$ = -880, -1603 kPa, are noticed along the axial depths of the foundation for the single U, double U-shaped pipe configurations, respectively. For the sandstone, the greatest values of the thermal stresses are $\sigma_{v,th}$ = -862, -1681 kPa, which are located at the same axial depths of the foundation and for the same type of the installed pipe configurations.

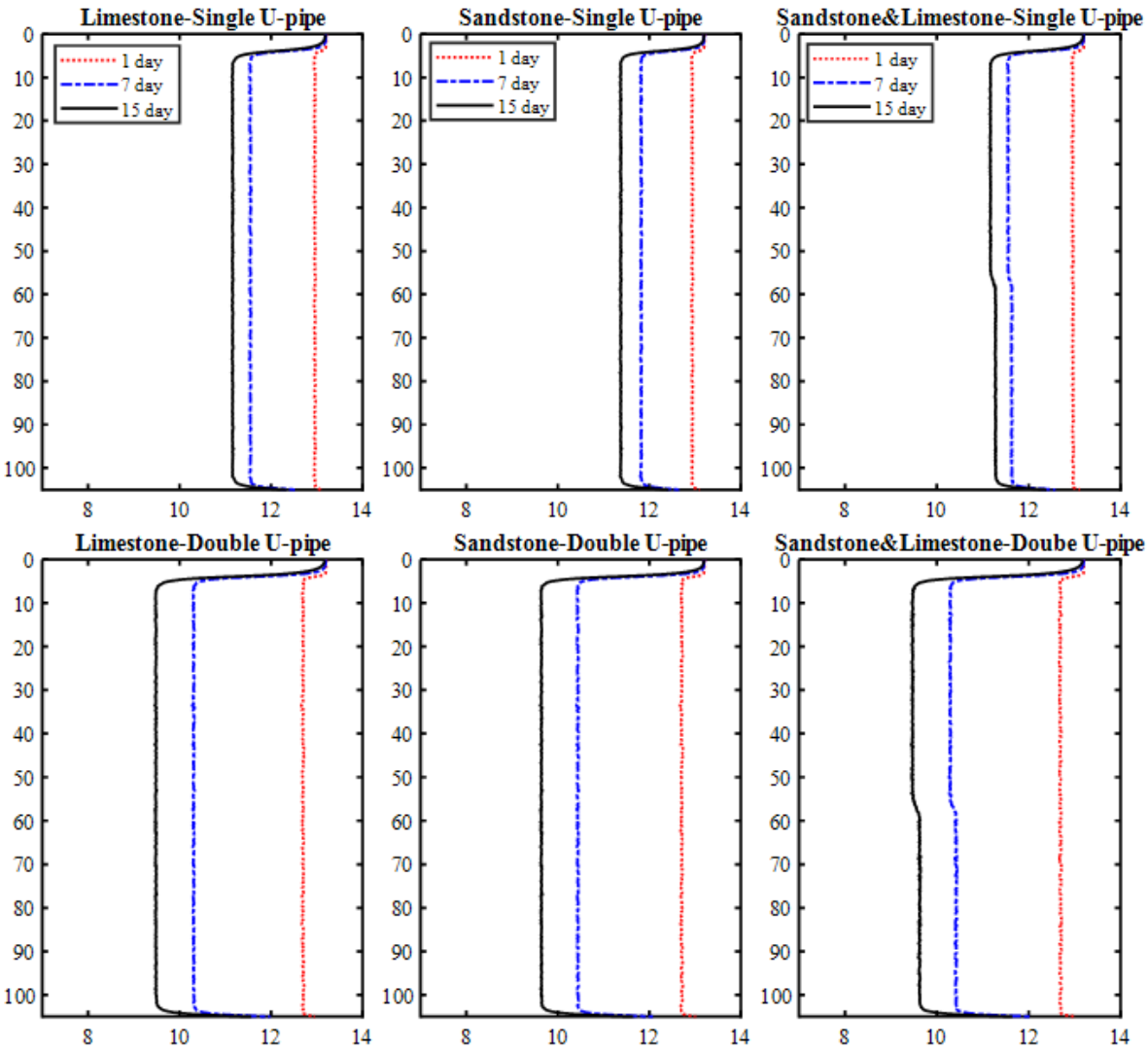

Figure 4.4. Axial temperature distributions for the U pipe (Top) and the doube-U pipe (Bottom) configurations embedded in limestone (Left), sandstone (Center), and a combination of both (Right) rock materials for domain (B).

In the the simulated cases, the thermal stress results are consistent with the previously observed data 4.1.1.4. The configurations of the pipes that led to the greatest negative temperature variations inside the pile were the configurations for which the greatest stresses were observed from the foundation thermal contractions. The obtained results of the magnitude of the stresses which are induced by the temperature variation in the energy pile equipped with the single U-shaped pipe configuration are close to the one characterizing the results obtained by Batini *et. al* [10] and Gashti *et. al* [29] for which a single energy pile that was studied in winter conditions with the same type of pipe configurations.

4.1.1.6. Distributions of the Displacement for Each Type of Pipe Configuration and Rock Materials for Domain (B)

Finally, Figure 4.3 shows the axial distribution of the vertical displacement. It has been observed that in this case and all the other simulated cases of domain (A), the displacements were consistent with the distributions of the temperature and stress profile. In all of the simulated cases, the results are close to the ones obtained by Batini et al [10] for the pile foundation equipped with a single U-pipe and double U-pipe configurations. The maximum effect of the cold flow within the tubes is observed for the pile foundation equipped with double U-pipe configuration. In contrast, the minimum effect is observed for the pile foundation equipped with a single U-pipe configuration. The maximum pile settlements dz_{th} = 0.9335, 1.713 mm are noticed when the pile foundation equipped with a single U-pipe and double U-pipe configurations, respectively, buried in limestone type of rock. Moreover, the maximum displacement of the pipe foundation where the energy pile that is buried in sandstone are dz_{th} = 0.57 and 1.11 mm for the same pipe configurations, respectively, and the maximum displacement for which the energy pile is buried sounding by the combination of both limestone and sandstone were dz_{th} = 0.55 and 1.03 mm observed the energy pile foundation which equipped with the single U, double U, respectively. Also, it was observed that the null point which describes the plane where zero thermally induced displacement happens in the foundation are similar to that results were obtained by Batini *et. al* [10] and

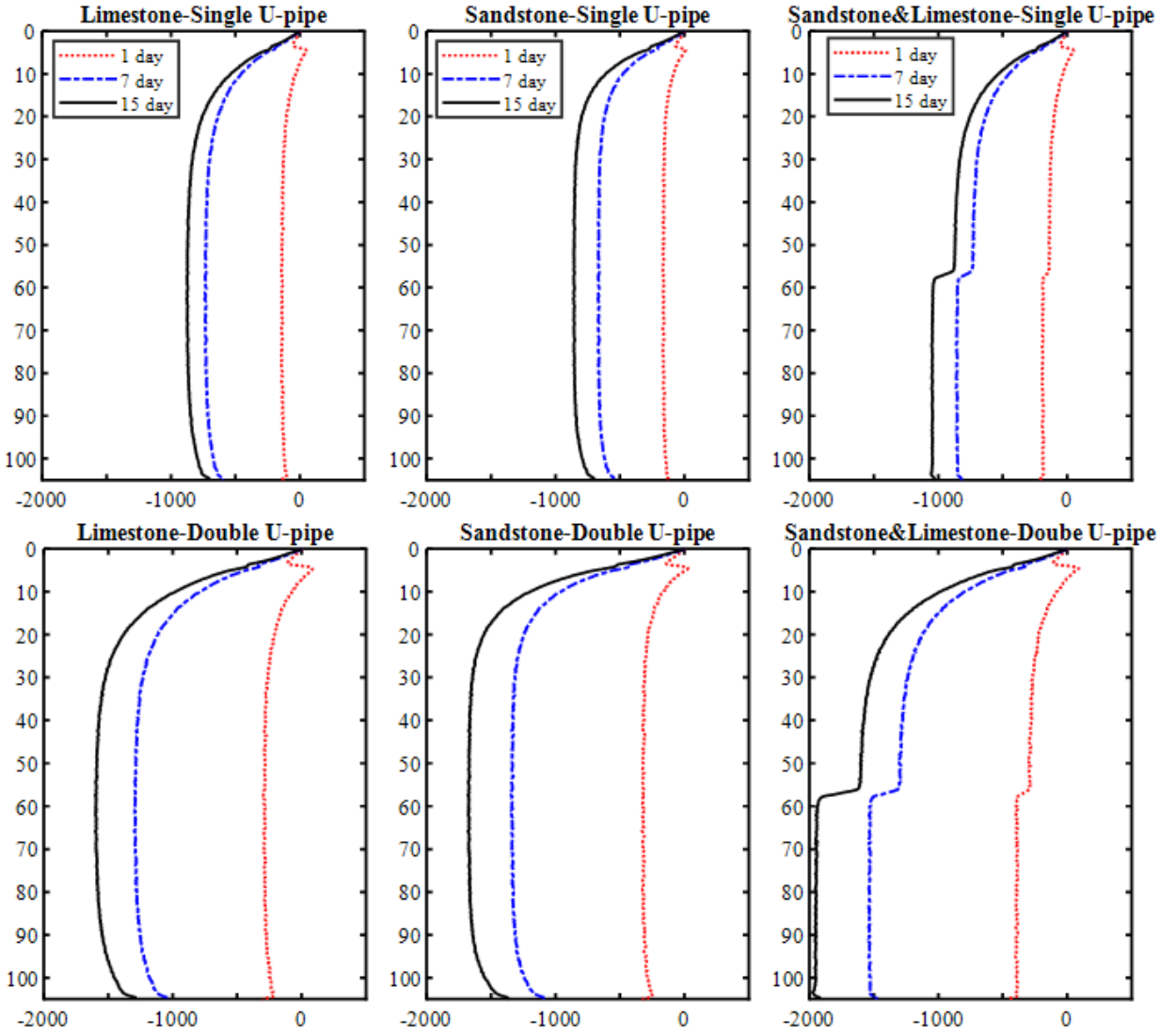

Figure 4.5. Axial distributions of the thermal vertical stresses for the U pipe (Top) and the doube-U pipe (Bottom) configurations embedded in limestone (Left), sandstone (Center), and a combination of both (Right) rock materials for domain (B).

Gashti *et. al* [29].

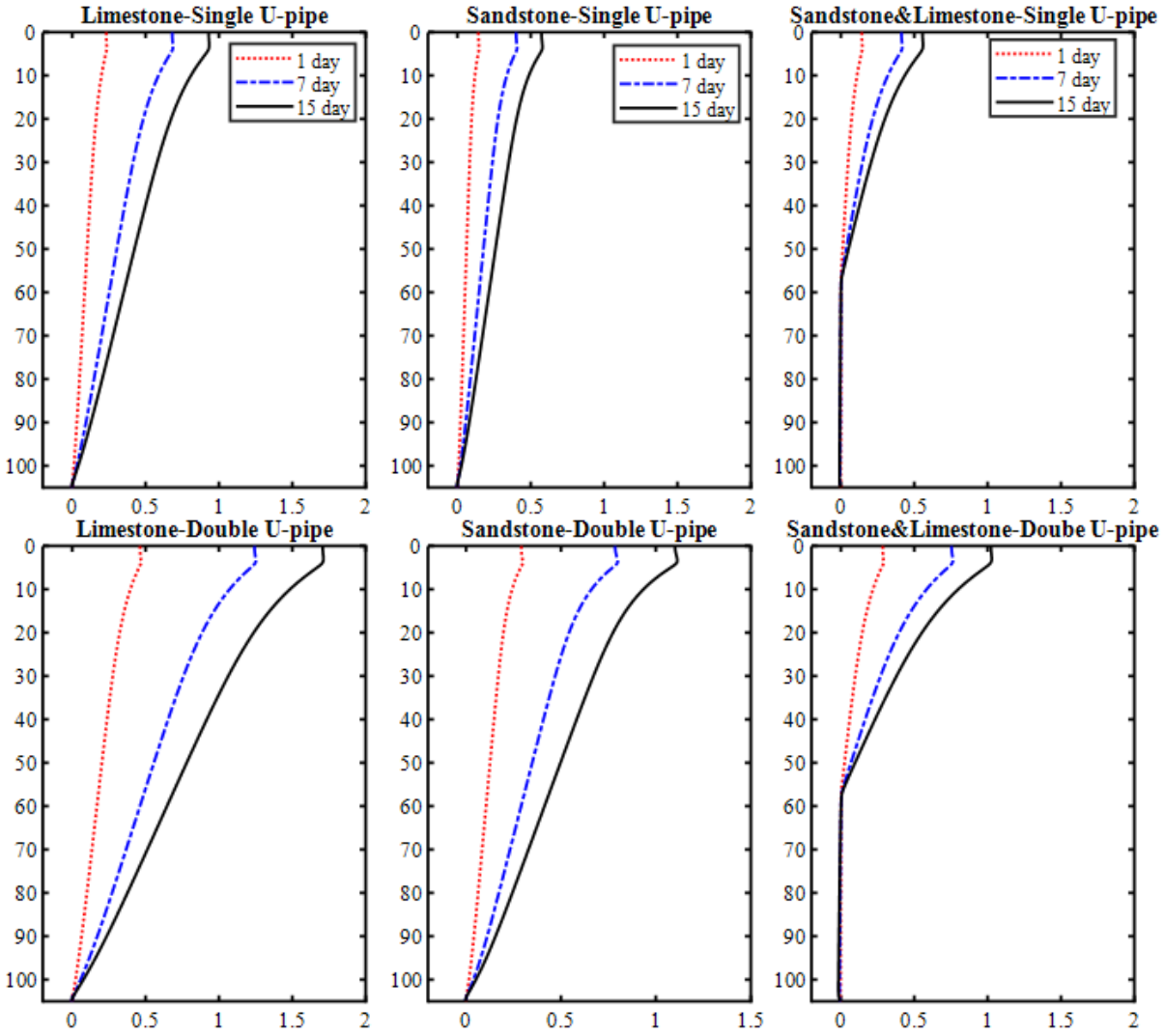

Figure 4.6. Axial distributions of the thermal vertical displacements for the U pipe (Top) and the doube-U pipe (Bottom) configurations embedded in limestone (Left), sandstone (Center), and a combination of both (Right) rock materials for domain (B).

4.1.2. Length Effect Comparison Between Domain A and B

The pile depth is extended for Domain B to observe the effect of the pile length on the thermal-mechanical response of the geothermal heat exchanger system. From the temperature axial distributions of the pile, minimal change was observed when the pipe length was

extended. This is due to the fact that the flow had already reached a fully developed state thermally for all days of operation and would not affect the pile temperature any further.

On the other hand, the thermal stresses increased when the pile depth is extended, as the stress build-up was not fully developed for domain A which had the maximum experienced stress at a depth of 30 meters. Extending the depth increased the stressed even further as seen from the stress values below a depth of 30 meters.

This increase in stress, and the doubling in the total length, contributed to displacements in domain B twice as much as those observed for domain. This ratio is explained due to the fact that the strain is accumulated along the pipe and results in twice the displacement when the pipe length is doubled.

4.1.3. Ground Thermal Power Extraction

The ground thermal power extraction for the considered pipe configurations, fluid properties, and the rock types are presented in Figure 4.7. A reduction of the thermal power extracted from the ground Q/H_{EP} is noticed with in the tests which was consistent with the temperature decreases happening at the interface of the rock-pile. However, after a week of the simulation operation, the time evolution of the extracted thermal power is close to the steady-state. Moreover, the double U-shaped pipe configuration provided the highest levels of energy extraction, where the lower amounts of energy is extracted from the ground through the single U-shaped pipe configuration. After 15 days of the simulation operation, the energy pile equipped with double U-shaped pipe configuration had a almost twice the heat transfer rate than what was obtained through a single U-shaped pipe configuration. Finally, when comparing these two types of pipe configurations, the double U-shaped pipe configuration should be considered the best in all of the simulated cases, because of its higher energy extraction.

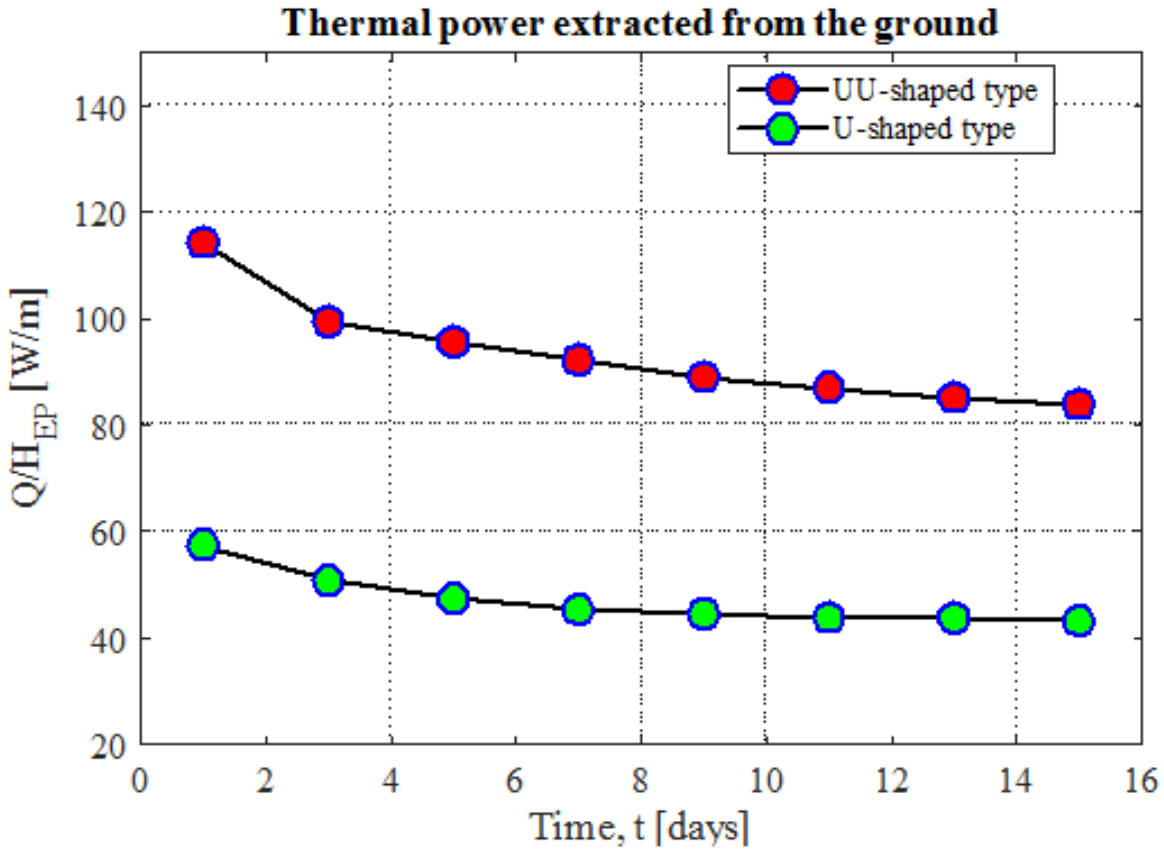

Figure 4.7. Trend of the thermal power extracted from the ground for the different pipe configurations.

Chapter 5

CONCLUSIONS AND FUTURE RESEARCH

5.1. Conclusion

Geothermal energy piles are a relatively new technology that couples the structural role of traditional pile foundations with heat exchangers to fulfill the required energy demand of buildings and infrastructures. These foundations are equipped with closed systems of pipes embedded in the concrete forming the pile. While connected to a heat pump, the fluid circulating inside these pipes provides the exchange of heat with the ground for heating and cooling purposes. At shallower depths of the ground, the temperature remains undisturbed the whole year and stays comparatively constant, warmer than the surrounding temperature in winter and cooler in summer, rendering the system thermal capacities beneficial for cooling and heating purposes. The application and integration of these systems into our present infrastructure is still in development as the behavior of such energy pile foundations, governed by their thermo-mechanical response, is still not fully understood.

This research presents a series of 3D finite element simulations that investigate the thermal and mechanical behavior of energy piles of different proposed design solutions under normal operating conditions. The heat exchange between the pile foundations and rock is investigated for power extraction capacity, temperature distributions, and the related stresses and displacements along the pile length. The four-meter pipe segment nearest to the ground surface is thermally insulated to limit the influence of external weather patterns on the heat exchange process and the energy pile's performance. The performance of two different pipe configurations (i.e. U-shaped and double U-shaped pipes) is studied within energy piles embedded in three different rock types (limestone, sandstone, and 50/50 combination). The study is performed in heating mode where cold water is introduced into the piles for heat

extraction, and the duration of operation extends over an initial transient thermal response, and up to a thermally quasi-steady state operation, which is reached after 15 days.

The outcomes from the conducted studies reveal that the different pipe configurations determine the behavior of the energy piles, leading to the following observations and conclusions:

- An increase in the axial distributions of vertical thermal stresses has been recorded when the pile equipped with double U-pipes is compared with that of the single U-pipe configuration, caused by the increase in temperature gradients between the added U-pipe and the surrounding foundation. Moreover, these stresses were extremely small and would unlikely cause any structural damage to the pile.

- The maximum value of the axial distributions of the thermal vertical displacements was observed when the pile foundation equipped with double U-pipes was buried in the limestone compared to sandstone, caused by the higher temperature gradients and thermal stresses. These displacements, however, were very small and would unlikely undermine the overall performance of the piles.

- The double U-shaped pipe configuration resulted in high heat transfer compared with that of a single U-shaped pipe configuration at the same flow rate, due to the added circulating cold fluid to extract heat from the energy pile.

- The highest cooling of the concrete with the maximum related stresses and displacement distributions occurred when the energy pile was equipped with the double U-shaped pipe configuration. This is because the double pipe configurations increased the temperature gradients in pile thus causing higher stresses.

- The thermal power extraction of the energy piles in rocky surrounding media (limestone and sandstone) is found to be greater than in soil media, as their conductivity (3-3.44 $W/m.K$) is higher than that of soil (1.11-1.8 $W/m.K$) as obtained from Batini *et. al* [10].

- The results demonstrated that sandstone induced a slightly higher heat exchange with the foundation even though its thermal conductivity is lower than limestone. This is due to the fact that sandstone has a higher heat capacity, and is denser than limestone. Thus the sandstone can store more energy and its temperature near the pile would not drop as much as the limestone would. The energy pile embedded in sandstone as a result gave 5% higher temperature when compared to limestone.

- After 15 days of operation, the energy pile equipped with double U-shaped pipe had approximately twice the heat transfer rate (84 W/m) compared to what was obtained through a single U-shaped pipe configuration (44 W/m).

- The model of energy pile in limestone resulted in higher stresses and displacements. This is because the energy pile embedded in limestone experience the more cooling compared to sandstone, which is due to the lower thermal conductivity of the limestone.

- The model results also show that increasing the length of the piles result in a slight increase in the developed thermal stresses, and a larger increase in vertical displacements proportional to the increase in length.

5.2. Future Research

- The study was performed only considering the heating mode for the energy pile. Future work should consider operation of the system in its cooling mode where warm water is introduced from the superstructure (building, infrastructure) into the energy pile to be cooled by the geothermal heat exchange.
- The thermal behavior of multi piles in long-term should be studied to assess the mutual heating between the piles which may reduce their performance and efficiency. This study would determine the optimal spacing of the piles and the best array configuration for their alignments.
- Future work should also consider the effect of increasing the circulating fluid velocity on the performance of geothermal energy pile. By varying the flow regime, the heat exchange within the pile could be enhanced.

BIBLIOGRAPHY

[1] Abdelaziz, S. L., Olgun, C. G., and Martin, II, J. Design and operational considerations of geothermal energy piles. In *Geo-Frontiers 2011: Advances in Geotechnical Engineering*. 2011, pp. 450–459.

[2] Abdelaziz, S. L., Olgun, C. G., and Martin II, J. R. Equivalent energy wave for long-term analysis of ground coupled heat exchangers. *Geothermics 53* (2015), 67–84.

[3] Al-Khoury, R., and Diersch, H.-J. *Computational Modeling of Shallow Geothermal Systems*, vol. 4. 2011.

[4] Allaerts, K., Coomans, M., and Salenbien, R. Hybrid ground-source heat pump system with active air source regeneration. *Energy Conversion and Management 90* (2015), 230–237.

[5] Armstead, H. Geothermal energy: Its past, present, and future contributions to the energy needs of man e. and fn spon. *London, UK* (1983).

[6] Association, G., et al. Thermal pile design, installation and materials standards. *Ground Source Heat Pump Association, Milton Keynes 82* (2012), 484.

[7] Aydin, M., and Sisman, A. Experimental and computational investigation of multi u-tube boreholes. *Applied energy 145* (2015), 163–171.

[8] Bandos, T. V., Campos-Celador, Á., López-González, L. M., and Sala-Lizarraga, J. M. Finite cylinder-source model for energy pile heat exchangers: Effects of thermal storage and vertical temperature variations. *Energy 78* (2014), 639–648.

[9] Bao, X., Memon, S. A., Yang, H., Dong, Z., and Cui, H. Thermal properties of cement-based composites for geothermal energy applications. *Materials 10*, 5 (2017), 462.

[10] Batini, N., Loria, A. F. R., Conti, P., Testi, D., Grassi, W., and Laloui, L. Energy and geotechnical behaviour of energy piles for different design solutions. *Applied Thermal Engineering 86* (2015), 199–213.

[11] Brandl, H. Energy piles for heating and cooling of buildings. In *Proceedings of 7th Int. Conf. Exhib. Piling and Deep Foundations, Vienna* (1998), pp. 341–346.

[12] Brandl, H. Energy foundations and other thermo-active ground structures. *Geotechnique 56*, 2 (2006), 81–122.

[13] Brandl, H. Thermo-active ground-source structures for heating and cooling. *Procedia Engineering 57* (2013), 9–18.

[14] Bullard, E. C. Historical introduction to terrestrial heat flow. *Terrestrial Heat Flow 8* (1965), 1–6.

[15] Buntebarth, G. *Geothermie: eine Einführung in die allgemeine und angewandte Wärmelehre des Erdkörpers*. Springer-Verlag, 2013.

[16] Carslaw, H., and Jaeger, J. *Conduction of heat in solids: Oxford Science Publications*. Oxford, England, 1959.

[17] Casarosa, C., Conti, P., Franco, A., Grassi, W., and Testi, D. Analysis of thermodynamic losses in ground source heat pumps and their influence on overall system performance. In *Journal of Physics: Conference Series* (2014), vol. 547, IOP Publishing, p. 012006.

[18] Comsol. *COMSOL Multiphysics Version 5.3a: User's Guide and Reference Manual*. Comsol Burlington, MA, USA, 2017.

[19] Di Donna, A., Loria, A. F. R., and Laloui, L. Numerical study of the response of a group of energy piles under different combinations of thermo-mechanical loads. *Computers and Geotechnics 72* (2016), 126–142.

[20] Dickson. *Geothermal Energy: Utilization and Technology, UNESCO Renewable Energy Series*.

[21] Dickson, M. H., and Fanelli, M. Geothermal r&d in developing countries: Africa, asia and the americas. *Geothermics 17*, 5-6 (1988), 815–877.

[22] Dincer, I., and Rosen, M. *Thermal energy storage: systems and applications*. John Wiley & Sons, 2002.

[23] Dupray, F., Laloui, L., and Kazangba, A. Numerical analysis of seasonal heat storage in an energy pile foundation. *Computers and Geotechnics 55* (2014), 67–77.

[24] Eskilson, P., and Claesson, J. Simulation model for thermally interacting heat extraction boreholes. *Numerical Heat Transfer 13*, 2 (1988), 149–165.

[25] Fadejev, J., and Kurnitski, J. Energy pile and heat pump modeling in whole building simulation model. 2nd ibpsa-england conference on building simulation and optimization. *London, United Kingdom* (2014), 23–24.

[26] Fadejev, J., and Kurnitski, J. Geothermal energy piles and boreholes design with heat pump in a whole building simulation software. *Energy and Buildings 106* (2015), 23–34.

[27] Fadejev, J., Simson, R., Kurnitski, J., and Haghighat, F. A review on energy piles design, sizing and modelling. *Energy 122* (2017), 390–407.

[28] Gao, J., Zhang, X., Liu, J., Li, K. S., and Yang, J. Thermal performance and ground temperature of vertical pile-foundation heat exchangers: A case study. *Applied Thermal Engineering 28*, 17-18 (2008), 2295–2304.

[29] Gashti, E. H. N., Malaska, M., and Kujala, K. Evaluation of thermo-mechanical behaviour of composite energy piles during heating/cooling operations. *Engineering structures 75* (2014), 363–373.

[30] Gashti, E. H. N., Uotinen, V.-M., and Kujala, K. Numerical modelling of thermal regimes in steel energy pile foundations: A case study. *Energy and buildings 69* (2014), 165–174.

[31] Ghasemi-Fare, O., and Basu, P. A practical heat transfer model for geothermal piles. *Energy and Buildings 66* (2013), 470–479.

[32] Girard, A., Gago, E. J., Muneer, T., and Caceres, G. Higher ground source heat pump cop in a residential building through the use of solar thermal collectors. *Renewable energy 80* (2015), 26–39.

[33] Gnielinski, V. New equations for heat and mass transfer in turbulent pipe and channel flow. *Int. Chem. Eng. 16*, 2 (1976), 359–368.

[34] Haaland, S. E. Simple and explicit formulas for the friction factor in turbulent pipe flow. *Journal of Fluids Engineering 105*, 1 (1983), 89–90.

[35] Hamada, Y., Saitoh, H., Nakamura, M., Kubota, H., and Ochifuji, K. Field performance of an energy pile system for space heating. *Energy and Buildings 39*, 5 (2007), 517–524.

[36] Hellström, G. *Ground heat storage: thermal analyses of duct storage systems*. Department of Mathematical Physics, Lund Univ., 1991.

[37] Hesaraki, A., Holmberg, S., and Haghighat, F. Seasonal thermal energy storage with heat pumps and low temperatures in building projects—a comparative review. *Renewable and Sustainable Energy Reviews 43* (2015), 1199–1213.

[38] Hu, P., Zha, J., Lei, F., Zhu, N., and Wu, T. A composite cylindrical model and its application in analysis of thermal response and performance for energy pile. *Energy and Buildings 84* (2014), 324–332.

[39] Huttrer, G. W. The status of world geothermal power generation 1995–2000. *Geothermics 30*, 1 (2001), 1–27.

[40] IGSHPA. Closed-loop/geothermal heat pump systems: Design and installation standards, 2007.

[41] Incropera, F. P., Lavine, A. S., Bergman, T. L., and DeWitt, D. P. *Fundamentals of heat and mass transfer*. Wiley, 2007.

[42] Kaltschmitt, M., Huenges, E., and Wolff, H. Energie aus erdwärme. *Dt. Verlag für Grundstoffindustrie, Stuttgart* (1999).

[43] Kavanaugh, S. P. Design of geothermal systems for commercial and institutional buildings. *GROUND-SOURCE HEAT PUMPS* (1997).

[44] Laloui, L., Nuth, M., and Vulliet, L. Experimental and numerical investigations of the behaviour of a heat exchanger pile. *International Journal for Numerical and Analytical Methods in Geomechanics 30*, 8 (2006), 763–781.

[45] Lazzari, S., Priarone, A., and Zanchini, E. Long-term performance of bhe (borehole heat exchanger) fields with negligible groundwater movement. *Energy 35*, 12 (2010), 4966–4974.

[46] Lee, C., and Lam, H. A simplified model of energy pile for ground-source heat pump systems. *Energy 55* (2013), 838–845.

[47] Lev Eppelbaum, Israel Kutasov, I. K. A. P. *Thermal Properties of Rocks and Density of Fluids*. 2014.

[48] Leventis, G., Principal, M., Poeppel, A., and Principal, S. Analysis and Design of the Kingdom Tower Piled Raft Foundation © d U. *CTBUH 2015*.

[49] Li, M., and Lai, A. C. Heat-source solutions to heat conduction in anisotropic media with application to pile and borehole ground heat exchangers. *Applied Energy 96* (2012), 451–458.

[50] Li, M., and Lai, A. C. Review of analytical models for heat transfer by vertical ground heat exchangers (ghes): A perspective of time and space scales. *Applied Energy 151* (2015), 178–191.

[51] Lindal, B. Industrial and other applications of geothermal energy. *Geothermal energy* (1973), 135–148.

[52] Loveridge, F., and Powrie, W. 2d thermal resistance of pile heat exchangers. *Geothermics 50* (2014), 122–135.

[53] Loveridge, F., and Powrie, W. G-functions for multiple interacting pile heat exchangers. *Energy 64* (2014), 747–757.

[54] Lubimova, E. Thermal history of the earth. *Washington DC American Geophysical Union Geophysical Monograph Series 13* (1969), 63–77.

[55] Lund, J. W., and Freeston, D. H. World-wide direct uses of geothermal energy 2000. *Geothermics 30*, 1 (2001), 29–68.

[56] Lund, J. W., Freeston, D. H., and Boyd, T. L. Direct utilization of geothermal energy 2010 worldwide review. *Geothermics 40*, 3 (2011), 159–180.

[57] Man, Y., Yang, H., Diao, N., Liu, J., and Fang, Z. A new model and analytical solutions for borehole and pile ground heat exchangers. *International Journal of Heat and Mass Transfer 53*, 13-14 (2010), 2593–2601.

[58] Mands, E., Sanner, B., and GbR, U. Shallow geothermal energy. *UBeG, Wetzlar, Germany* (2005).

[59] Marcotte, D., and Pasquier, P. On the estimation of thermal resistance in borehole thermal conductivity test. *Renewable energy 33*, 11 (2008), 2407–2415.

[60] Miyara, A., Tsubaki, K., Inoue, S., Yoshida, K., et al. Experimental study of several types of ground heat exchanger using a steel pile foundation. *Renewable Energy 36*, 2 (2011), 764–771.

[61] Olgun, C. G., Ozudogru, T. Y., Abdelaziz, S. L., and Senol, A. Long-term performance of heat exchanger piles. *Acta Geotechnica 10*, 5 (2015), 553–569.

[62] Olgun, C. G., Ozudogru, T. Y., and Arson, C. Thermo-mechanical radial expansion of heat exchanger piles and possible effects on contact pressures at pile-soil interface.

[63] Ozudogru, T. Y., Olgun, C. G., and Arson, C. F. Analysis of friction induced thermo-mechanical stresses on a heat exchanger pile in isothermal soil. *Geotechnical and Geological Engineering 33*, 2 (2015), 357–371.

[64] Pahud, D., and Hubbuch, M. Measured thermal performances of the energy pile system of the dock midfield at zürich airport.

[65] Park, S., Lee, D., Choi, H.-J., Jung, K., and Choi, H. Relative constructability and thermal performance of cast-in-place concrete energy pile: Coil-type ghex (ground heat exchanger). *Energy 81* (2015), 56–66.

[66] Recast, E. Directive 2010/31/eu of the european parliament and of the council of 19 may 2010 on the energy performance of buildings (recast). *Official Journal of the European Union 18*, 06 (2010), 2010.

[67] Reda, F. Long term performance of different sagshp solutions for residential energy supply in finland. *Applied Energy 144* (2015), 31–50.

[68] Rotta Loria, A. F., Donna, A. D., and Laloui, L. Numerical study on the suitability of centrifuge testing for capturing the thermal-induced mechanical behavior of energy piles. *Journal of Geotechnical and Geoenvironmental Engineering 141*, 10 (2015), 04015042.

[69] Rybach, L., and Eugster, W. J. Sustainability aspects of geothermal heat pump operation, with experience from switzerland. *Geothermics 39*, 4 (2010), 365–369.

[70] Saggu, R., and Chakraborty, T. Cyclic thermo-mechanical analysis of energy piles in sand. *Geotechnical and Geological Engineering 33*, 2 (2015), 321–342.

[71] Sailer, E., Taborda, D. M., and Keirstead, J. Assessment of design procedures for vertical borehole heat exchangers.

[72] Sanner, B. Shallow geothermal energy. *Geo-Heat Center Bulletin* (2001).

[73] Sanner, B., Systems, O., Systems, C., and Pumps, G.-s. H. Shallow geothermal energy. *Geo-Heat Center Bulletin*, June (2001), 19–26.

[74] Serway, R. A. *Overhead Transparencies Physics for Scientists and Engineers*. Saunders College, 1996.

[75] Stacey, F. D., and Loper, D. E. Thermal history of the earth: a corollary concerning non-linear mantle rheology. *Physics of the earth and planetary interiors 53*, 1-2 (1988), 167–174.

[76] Standard, M. I. Mis 3005 issue 4.0. requirements for contractors undertaking the supply, design, installation, set to work, commissioning and handover of microgeneration heat pump systems. *London, UK* (2013).

[77] Suryatriyastuti, M., Mroueh, H., and Burlon, S. Understanding the temperature-induced mechanical behaviour of energy pile foundations. *Renewable and sustainable energy reviews 16*, 5 (2012), 3344–3354.

[78] Tassou, S., Christodoulides, P., and Panayides, I. Measurement and analysis of thermal properties of rocks for the compilation of geothermal maps of Cyprus. 418–429.

[79] VDI, V. 4640-thermal use of underground. *Blatt 1: Fundamentals, approvals, environmental aspects* (2010).

[80] Wang, D., Lu, L., Zhang, W., and Cui, P. Numerical and analytical analysis of groundwater influence on the pile geothermal heat exchanger with cast-in spiral coils. *Applied energy 160* (2015), 705–714.

[81] Waples, D. W., and Waples, J. S. A Review and Evaluation of Specific Heat Capacities of Rocks , Minerals , and Subsurface Fluids . Part 1 : Minerals and Nonporous Rocks.

[82] Yang, H., Cui, P., and Fang, Z. Vertical-borehole ground-coupled heat pumps: A review of models and systems. *Applied energy 87*, 1 (2010), 16–27.

[83] Zarrella, A., De Carli, M., and Galgaro, A. Thermal performance of two types of energy foundation pile: helical pipe and triple u-tube. *Applied Thermal Engineering 61*, 2 (2013), 301–310.

[84] Zeng, H., Diao, N., and Fang, Z. A finite line-source model for boreholes in geothermal heat exchangers. *Heat Transfer—Asian Research: Co-sponsored by the Society of Chemical Engineers of Japan and the Heat Transfer Division of ASME 31*, 7 (2002), 558–567.

[85] Zhang, C., Guo, Z., Liu, Y., Cong, X., and Peng, D. A review on thermal response test of ground-coupled heat pump systems. *Renewable and Sustainable Energy Reviews 40* (2014), 851–867.

[86] Zhang, W., Yang, H., Lu, L., and Fang, Z. The analysis on solid cylindrical heat source model of foundation pile ground heat exchangers with groundwater flow. *Energy 55* (2013), 417–425.